

The University of Maine

DigitalCommons@UMaine

Electronic Theses and Dissertations

Fogler Library

12-2019

Three-dimensional Analytical Model of Tidal Flow in the Damariscotta River Estuary, ME

Stephanie L. Ayres
University of Maine

Follow this and additional works at: <https://digitalcommons.library.umaine.edu/etd>



Part of the [Mathematics Commons](#)

Recommended Citation

Ayres, Stephanie L., "Three-dimensional Analytical Model of Tidal Flow in the Damariscotta River Estuary, ME" (2019). *Electronic Theses and Dissertations*. 3152.
<https://digitalcommons.library.umaine.edu/etd/3152>

This Open-Access Thesis is brought to you for free and open access by DigitalCommons@UMaine. It has been accepted for inclusion in Electronic Theses and Dissertations by an authorized administrator of DigitalCommons@UMaine. For more information, please contact um.library.technical.services@maine.edu.

**THREE-DIMENSIONAL ANALYTICAL MODEL OF TIDAL FLOW IN THE
DAMARISCOTTA RIVER ESTUARY, ME**

By

Stephanie Lauren Ayres

B.S. Marine Science, University of South Carolina, 2014

M.S. Oceanography, University of Maine, 2017

A THESIS

Submitted in Partial Fulfillment of the

Requirements for the Degree of

Master of Arts

(in Mathematics)

The Graduate School

The University of Maine

December 2019

Advisory Committee:

Thomas Bellsky, Assistant Professor of Mathematics, Advisor

Lauren Ross, Assistant Professor of Civil Engineering

Peter Stechlinski, Assistant Professor of Mathematics

Robert Franzosa, Professor of Mathematics

THREE-DIMENSIONAL ANALYTICAL MODEL OF TIDAL FLOW IN THE DAMARISCOTTA RIVER ESTUARY, ME

By Stephanie Lauren Ayres

Thesis Advisor: Thomas Bellsky

An Abstract of the Thesis Presented
in Partial Fulfillment of the Requirements for the
Degree of Master of Arts
(in Mathematics)
December 2019

Estuaries are coastal bodies of water subjected to strong tidal influence and characterized by their morphology, tidal dynamics, topography, and stratification [3, 14]. Tidal flow is critically important to the water circulation, nutrient influx, and sediment transport in or out of an estuary. However, tidal asymmetry enhanced by estuary shape and nonlinear processes can lead to complications in estuarine flow. Analytical models are used to systematically study tidal flow within an estuary. Previous studies have derived analytical models of varying complexity and applied them to investigate tidal and residual flow [6, 15, 4, 12]. This thesis derives a three-dimensional analytical model with a perturbation expansion of the Navier-Stokes equations in the shallow water limit, modified from [4]. The resulting zero-order solution is analyzed to provide insight into the tidal flow of the Damariscotta River estuary. The Damariscotta River is a tidally-dominated, well-mixed estuary located on the coast of Maine. Despite its importance to local aquaculture, few studies have been conducted within the estuary [9, 8, 7]. This thesis is an exploratory study providing further understanding of the tidal flow dynamics of the Damariscotta River estuary.

The water level elevation and three-dimensional tidal flow velocity are presented, and sensitivity to changes in friction and width convergence are studied by altering their respective parameters, vertical eddy viscosity and width convergence factor. Water level elevation amplitude increases along-channel due to amplification from width convergence and, contra rily, along-channel velocity amplitude decreases along-channel due to friction, which suggests that width convergence dominates friction in determining water elevation, but friction has greater influence over velocity. This could be the result of the model assuming constant friction. Lateral velocities exhibited a two-cell structure with flow of the near-surface cell and the near-bottom cell in opposite directions. Results of the model compared well to previous studies within the estuary [7] and to the Upper Ems estuary [4], which has similar dynamics as the Damariscotta estuary although important morphological distinctions should be noted. Tidal asymmetry and variable friction within the estuary were not studied in this thesis, as non-linear terms were dropped in governing equations and vertical eddy viscosity was assumed to be constant. Furthermore, the model considers the zero-order solution and is unable to study residual flow in the estuary. Future work should investigate tidal asymmetry and residual flow in the Damariscotta estuary, while considering a more complicated friction regime.

DEDICATION

To Tyler, for always being supportive.

ACKNOWLEDGEMENTS

I would like to thank my advisor, Thomas Bellsky, for his guidance throughout this project. I would also like to thank committee member Lauren Ross for her crucial insight into estuarine dynamics. Additional thanks to Robert Franzosa and Peter Stechlinski for their questions and comments throughout this process, which greatly enhanced understanding and discussion.

TABLE OF CONTENTS

DEDICATION	ii
ACKNOWLEDGEMENTS	iii
LIST OF TABLES	vi
LIST OF FIGURES	vii
Chapter	
1. INTRODUCTION	1
1.1 Classifications of Estuaries	2
1.2 Tides in Estuaries.....	6
1.2.1 Importance	6
1.2.2 Tidal asymmetry	6
1.2.3 Analytical Modeling of Estuaries	8
1.2.3.1 Previous Analytical Studies of Estuaries	8
1.3 Research Gaps and Thesis Objectives	10
2. METHODS	11
2.1 Model Derivation	11
2.1.1 Equations and Variables	11
2.1.1.1 Integrated Continuity Equation	14
2.1.2 Non-dimensionalization	16
2.1.3 Perturbation Expansion	23

2.1.4	Zero-order Problem and Solution.....	25
2.1.4.1	Along-channel Velocity	28
2.1.4.2	Water Level.....	30
2.1.4.3	Across-Channel Velocity	33
2.1.4.4	Vertical Velocity.....	48
3.	RESULTS AND DISCUSSION	54
3.1	Water Elevation.....	58
3.2	Velocity	59
3.3	Sensitivity to Friction and Width Convergence.....	64
3.4	Significance, Limitations, and Future Work.....	67
3.5	Conclusions.....	67
	REFERENCES	69
	BIOGRAPHY OF THE AUTHOR	71

LIST OF TABLES

Table 2.1	Parameter values for the Damariscotta River estuary	12
-----------	---	----

LIST OF FIGURES

Figure 1.1	Characteristics of a standing and progressive wave and a wave with characteristics of both [3].....	3
Figure 1.2	Tidal amplitude, tidal current velocity, and estuary shape of hypersynchronous (a), synchronous(b), and hyposynchronous (c) estuaries [10].	5
Figure 1.3	Vertical salinity structure and currents in salt-wedge (top left), weakly-stratified (top right), strongly stratified (bottom left), and well-mixed (bottom right) estuaries [14].	6
Figure 1.4	Tidal current velocity over a tidal cycle for flood-dominate (a) and ebb-dominate(b) estuaries.....	7
Figure 2.1	Model estuary schematic [4].....	12
Figure 3.1	Location and satellite (Google Earth) image of the study area: the Damariscotta River Estuary, ME.	57
Figure 3.2	Amplitude and phase of water level elevation (η) as a function of along-channel distance into the estuary, x	58
Figure 3.3	Amplitude and phase of along-channel velocity, u , at the center, surface of the channel as a function of distance along the estuary, x	60
Figure 3.4	Amplitude (a, c, e) and phase (b, d, f) of along-channel velocity, u , at one-quarter length (top row) into the estuary, mid-estuary (middle row), and three-quarters into the estuary (bottom row) for the estuary cross-section.....	62

Figure 3.5	Along-channel velocity at one-quarter length (left) and half-length (right) into the estuary during several times during the tidal cycle: $t = 0$ (a,b), $t = 6$ h(c,d), $t = 9$ h (e,f), $t = 11.5$ h (g,h).....	63
Figure 3.6	Amplitude of water level (η) for vertical eddy viscosity, A_v , values of 10^{-1} (a) and 10^{-4} (b), representative of strong and weak friction, respectively.	65
Figure 3.7	Amplitude of along-channel velocity (u) for vertical eddy viscosity, A_v , values of 10^{-1} (a) and 10^{-4} (b), representative of strong and weak friction, respectively.	66
Figure 3.8	Amplitude of water level (a) and along-channel velocity (b) for a channel with stronger width convergence, $\mu = 3$	66

CHAPTER 1

INTRODUCTION

Estuaries are coastal bodies of water, commonly formed at the mouths of rivers, within which seawater is diluted with freshwater. However, there are numerous formal definitions of an estuary. The most commonly cited is that of Cameron & Pritchard (1963), which states an estuary is a semi-enclosed coastal body of water which has a free connection to the open ocean and within which sea water is measurably diluted with freshwater derived from land drainage [1]. Alternative definitions have been based upon the influence of the tides or the source of sediments within an estuary. The morphology of an estuary may change over time if either the flow entering or exiting the estuary is stronger than the other, a phenomena known as tidal asymmetry that will be described in further detail in a later section. Estuaries are initially sediment traps until an equilibrium is reached between sediment inputs after which the physical processes of the estuary and the morphology of the estuary is relatively stable with time [3]. Estuaries are sensitive to increases in sea level and changes in estuary shape.

Flow within an estuary is subjected to strong tidal influence. Tides are created by the gravitational forces of the moon and sun acting upon the earth, with the moon being the dominant force due to its proximity. The result is a pattern of flood, when water moves landward, ebb, when water moves seaward, and slack, periods of very weak or no current occurring between the flood and ebb stages. There are hundreds of tidal frequencies with diurnal, semi-diurnal, and mixed. Diurnal tide has a single occurrence of high and low tide per day, semi-diurnal tide has two periods high tide and low tide per day, and mixed tide has two periods high and low tide, which are measurably different. The magnitude and frequency of the tide depends on the relative positions of the sun and moon. Twice during each lunar month, there are spring tides, when the sun and moon are aligned, which creates high tides which are higher than normal and low tides that are lower than normal.

Neap tides occur when the moon and sun are perpendicular, creating high tides that are lower than normal and low tides that are higher than normal. The tide is considered a combination of harmonic tidal constituents and the principal components are M2, S2, O1, K1, and N2. The M2 constituent is the principal lunar semidiurnal with a period of 12.42 hours, the S2 constituent is the principal solar semidiurnal constituent with a period of 12 hours, the O1 is the principal lunar diurnal constituent with a period of 25.82 hours, the K1 is the lunisolar diurnal constituent with a period of 23.92 hours, and the N2 is the lunar elliptic semidiurnal constituent with a period of 12.66 hours.

The tidal wave travels as a shallow water wave toward the head of the estuary. Shallow water waves occur where the water depth is much less than half the tidal wavelength. Without friction, the wave will be reflected, and it will interfere with the next wave entering the estuary [3]. The tidal wave is a standing wave with an antinode, the point where the amplitude of the wave is maximum, at the head of the estuary and a node at one quarter the wavelength distance into the estuary. The tidal amplitude is ninety degrees out of the phase with current velocity, which means there is a time lag between maximum water height and maximum velocity [3]. If completely dissipated by friction, the tidal wave becomes a progressive wave. Amplitude of the tide and the magnitude of the tidal current decrease towards the head of the estuary, and the tidal amplitude is in phase with current velocity [3]. Figure 1.1 illustrates the distinction between a standing and progressive wave, as well as a wave with both characteristics which is common in estuaries [3].

1.1 Classifications of Estuaries

Estuaries can be classified in many ways, for example, based upon the characteristics of their topography, tidal flow, morphology, and stratification [3, 14]. Most estuaries can be divided into three topographic cases: coastal plain (drowned river valley), fjord, and bar-built [11]. Coastal plain estuaries formed over a period of rapid sea level rise, which occurred at the end of the last glacial period. Their topography resembles that of a river

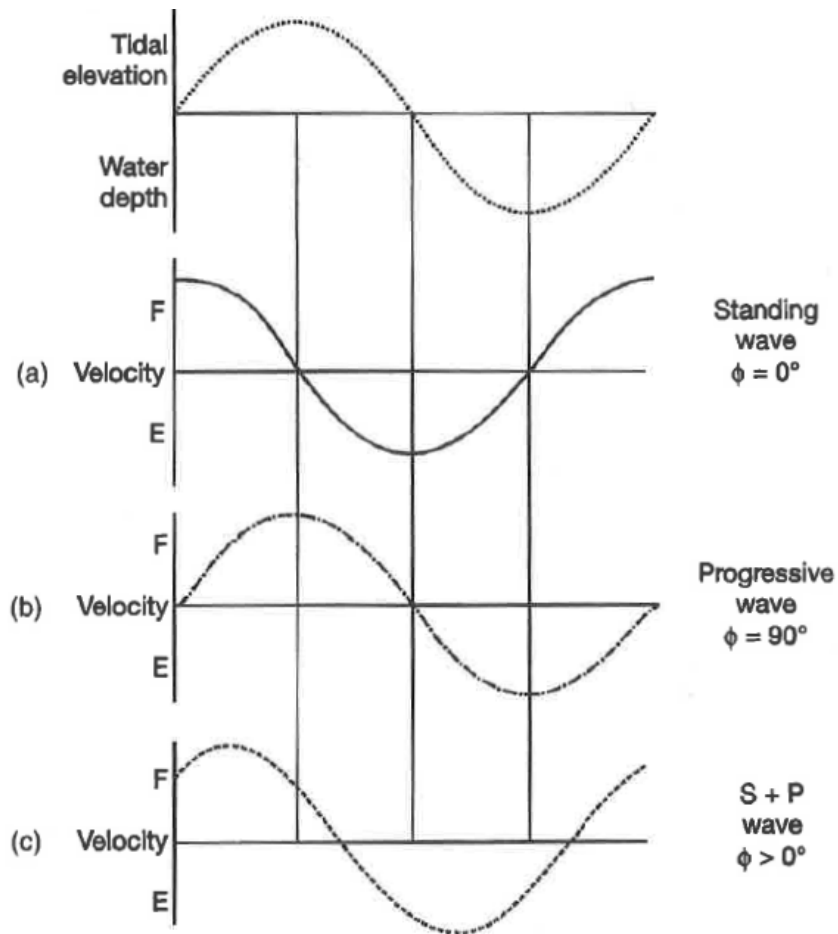


Figure 1.1. Characteristics of a standing and progressive wave and a wave with characteristics of both [3].

valley due to insufficient sedimentation [3]. These estuaries are often relatively shallow, with 30 m maximum depth and triangular cross-sections. The estuary bottom may be composed of mud or sand. In some cases, width increases exponentially towards the mouth (seaward end of estuary). Generally, river flow is weak in comparison to the tidal flow. Chesapeake Bay, USA is an example of a coastal plain estuary. Fjords formed in areas covered by progressing glaciers, which deepened and widened pre-existing river valleys [3]. They are deep and straight, although sharp bends may occur, with rectangular cross-sections. Unlike coastal plain estuaries, fjords are usually deeper than they are wide. They have rocky bottoms and occur primarily at high latitudes. Commonly present at the mouth are shallower sills which restrict the connection to the sea, and, thus, river flow is

stronger than tidal flow. Bar-built estuaries are coastal plain estuaries which have a characteristic bar across the mouth built by coastal sedimentation [3]. These estuaries are shallow with lagoons occurring near the mouth and have a relatively small range in tides. The mouth of the estuary is restricted by the bar, creating high current velocities that rapidly decrease within the estuary. River flow is generally stronger than tidal flow in a bar-built estuary.

Estuaries can also be classified by the size of their tidal range, the difference in water height of successive high and low tides. Microtidal estuaries have a tidal range less than 2 meters, mesotidal have a tidal range of 2 to 4 meters, macrotidal have a tidal range of 4 to 6 meters, and hypertidal have a tidal range greater than 6 meters. The magnitude of the tidal range and the strength of the tidal currents is dependent on the interaction of the tidal wave with the estuary's morphology, specifically the relative influences of width convergence and friction [3]. Convergence without friction compresses the tidal wave laterally, forcing an amplification of the tidal range and current velocity. Friction, on the other hand, dampens the tidal wave and reduces the tidal range and current velocity. Estuaries are considered hypersynchronous if convergence exceeds friction, synchronous if friction and convergence have equal influence on the tides, and hyposynchronous if friction exceeds convergence (Fig. 1.2). In hypersynchronous estuaries, the tidal range and currents increase towards the head until the riverine section, where convergence diminishes and friction becomes important, reducing the tide [3]. In synchronous estuaries, the tidal range is constant until the riverine section. In hyposynchronous estuaries, the tidal range and currents diminish along the estuary towards the head [3]. Hyposynchronous estuaries tend to be wave-dominated, whereas hypersynchronous estuaries tend to be tidal-dominated.

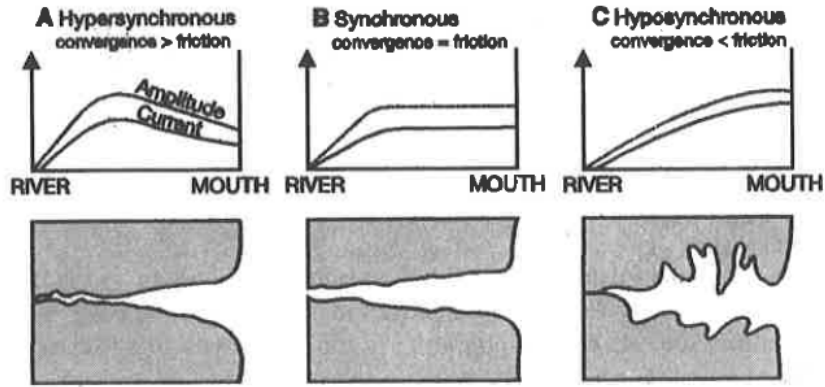


Figure 1.2. Tidal amplitude, tidal current velocity, and estuary shape of hypersynchronous (a), synchronous(b), and hyposynchronous (c) estuaries [10].

In terms of salinity and density stratification, estuaries are classified as salt-wedge, strongly (highly) stratified, weakly stratified, and well-mixed, Figure 1.3 [3, 14]. Salt-wedge estuaries are strongly stratified with a wedge-shaped saltwater intrusion near the bottom, resulting from large river discharge into the estuary and weak tidal influence [3, 14]. The characteristic of the salt-wedge change during the tidal cycle. Mean flow in salt-wedge type estuaries is dominated by outflow in most of the the water column with weak inflow near the bottom [14]. Strongly stratified estuaries are similar to salt-wedge, but remain stratified throughout the tidal cycle. Fjords are strongly stratified. Inflow is stronger than in salt-wedge estuaries, but overpowered by outflow, creating strong vertical density gradients. Weakly stratified estuaries, also known as partially-mixed, have moderate to strong tidal influence compared to weak to moderate river influence. Vertical salinity gradients are weak. Well-mixed estuaries are nearly vertically uniform in terms of salinity, due to strong mixing caused by strong tidal influence.

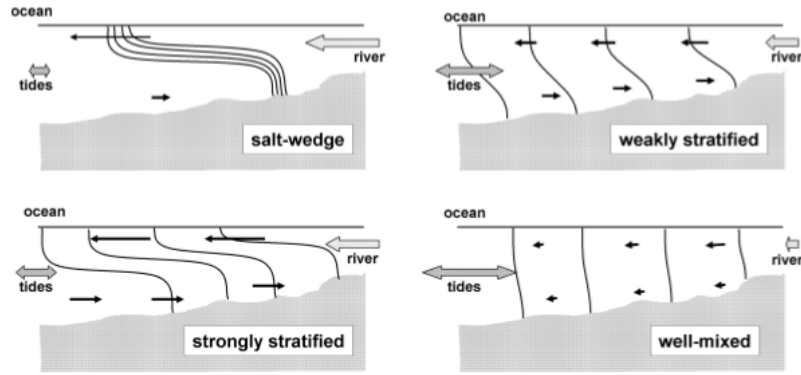


Figure 1.3. Vertical salinity structure and currents in salt-wedge (top left), weakly-stratified (top right), strongly stratified (bottom left), and well-mixed (bottom right) estuaries [14].

1.2 Tides in Estuaries

1.2.1 Importance

The tides are critically important to estuaries. They are responsible for the flushing of water in and out of the estuary at the mouth. This exchange brings in nutrients, enriching these environments, and controls the sediment transport in or out of the estuary. In many estuaries, the tides drive circulation. Understanding tidal flow can provide insight into the overall patterns of water movement in the estuary.

1.2.2 Tidal asymmetry

Tidal distortion, which creates asymmetric tides, occurs over the continental shelf and is further enhanced by estuary processes and morphology [2]. The elevation tidal amplitude ratio, the ratio of the amplitude of M_4 tidal constituent to the amplitude of the M_2 tidal constituent, is used to determine the nature and strength of tidal asymmetry of an estuary [5].

Large variations in water depth during the tidal cycle cause the crest of the tidal wave to travel faster than the trough and the crest may partially overtake the trough [3]. This leads to shorter flood and longer ebb stages of the tidal cycle with maximum current

velocity occurring during the flood stage (Fig. 1.4). Non-linear processes, such as advective accelerations, increase the duration of slack period before ebb and ebb currents are faster than flood currents [2]. These processes have a smaller effect in short estuaries which have a length much smaller than their tidal wavelength. Bottom friction has an increased effect in shallow estuaries and during low tide. During low-tide, friction slows water movement, leading to an increased delay of low tide along the estuary than that of high tide. Current velocities are slightly faster during flood, opposite to the effect of other non-linear terms. The combination of these effects results in an estuary with shorter flood stage with faster current, and the estuary is considered flood-dominated. Sediment transport is greater into the estuary and, therefore, flood-dominated estuaries tend to be shallow.

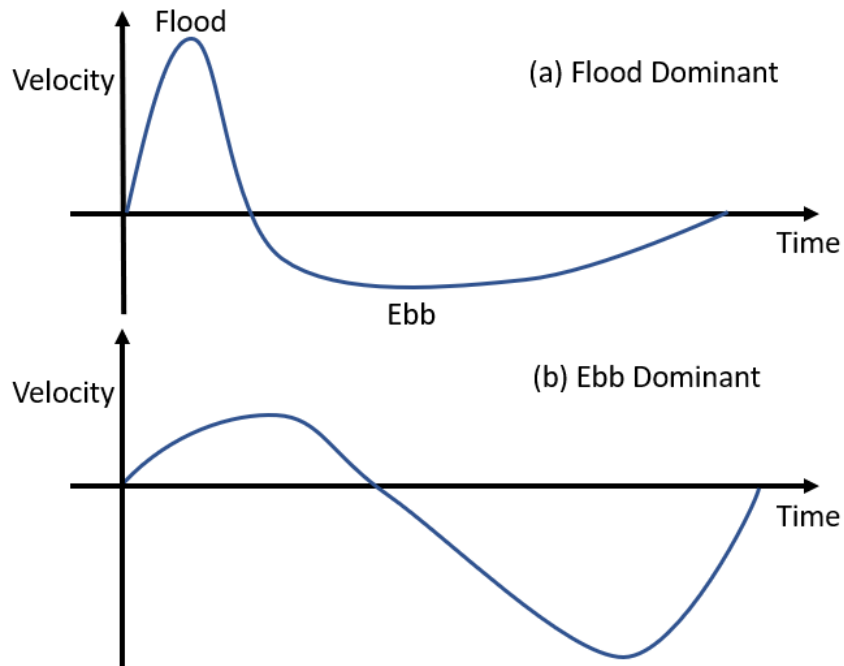


Figure 1.4. Tidal current velocity over a tidal cycle for flood-dominant (a) and ebb-dominant (b) estuaries. Tidal current velocity over a tidal cycle for flood-dominant (a) and ebb-dominant (b) estuaries.

Contrarily, interactions between the deep channel and shallow tidal storage (e.g. tidal flats, marshes) portions of the estuary and variations in friction can create ebb-dominance.

The presence of large tidal flats enhances ebb currents [13]. The time lag in the elevation of ocean water levels and that of the estuary is less during low tide. The curve of the tidal wave steepens during ebb, increasing ebb current velocities [3]. Changes in cross-sectional area at the mouth during the tidal cycle enhance this process.

1.2.3 Analytical Modeling of Estuaries

Estuarine circulation has been studied through observational and theoretical studies. Although observational studies provide a detailed, accurate investigation of flow in an estuary, they require hours of field work, which is impractical for estuaries in remote locations. Theoretical studies involving mathematical modeling allow researchers to study estuaries without these restrictions. Numerical models are used to approximate flow within an estuary, while analytical models, derived through algebraic methods, are used to systematically study approximate flow within an estuary. In analytical models, estuary processes can be isolated and parameters, e.g. width convergence, can be adjusted to study how changes affect the flow. This allows an analytical model to be applied to several estuaries with similar dynamics by changing model parameters. The complicated shape and curvature of estuaries is simplified to that of a prism and friction is considered to be constant or linear with depth to maintain analytic solutions. Despite these limitations, results from analytical models provide crucial understanding and compare reasonably well with observations. The following is a discussion of important results from previous analytical studies of varying complexity.

1.2.3.1 Previous Analytical Studies of Estuaries

Friedrichs & Aubrey (1994) developed theory on tides in shallow, convergent estuaries by deriving a one-dimensional analytical model. Contrary to previous work, in which water motion was described by second-order wave equations, their improved scaling resulted in a first-order wave equation which describes uni-directional wave progression, indicating there is no reflected wave present. The tidal wave had characteristics of both standing and

progressive wave, and tidal motion was heavily dependent on friction [6]. Although their work provided fundamental understanding of tidal motion in convergent estuaries, one-dimensional models give a limited view of three-dimensional estuaries.

With a three-dimensional analytical model derived from a perturbation expansion of the horizontal Reynolds averaged Navier-Stokes equations in the shallow water limit, Winant (2007) studied tidal flow in a generalized elongated basin with width less than its external Rossby radius. The study focused on the effects of rotation and friction on tidal flow. Rotation and lateral sea-level gradients were found to drive lateral circulation, the strength of which was dependent on friction [15]. Across-channel (lateral) flow was small in comparison to along-channel (longitudinal) flow when friction was strong, but when friction is weak to moderate, lateral flow is of comparable magnitudes to along-channel velocities.

Ross et al. (2014) examines tidal dynamics in a narrow, deep, fjord-like basin using a three-dimensional analytical model. They argued that the classical-view of fjord systems, horizontal density gradients in a thin upper layer of the water column drive flow and currents below the layer are weak, was an oversimplification. Independent of width convergence, there was a slight increase in tidal wave amplitude from mouth to head, indicative of a standing wave system. Although decreasing friction caused increasing amplification of the tidal wave, this effect was less pronounced if width convergence was strong. For fjords with weak width convergence, the frictional boundary layer is much less than the water depth causing the subsurface maximum and an increase in tidal amplitude with decreasing depth.

Using similar methodology as Winant (2007), Ensing et al. (2015) examines the effects of cross-section shape and anthropogenic impacts on the tidal flow of a well-mixed estuary. The study area was the Upper Ems, Netherlands. Their results supported claims in Winant (2007) that lateral flow was found to be dominated by rotation and lateral density gradients. Laterally skewing the bottom profile enhanced lateral flow [4]. The amplitude increased due to width convergence, but was not impacted by lateral skewness in the

bottom profile. Given symmetric bottom profile, lateral velocities were laterally antisymmetric, becoming asymmetric when the profile is skewed [4].

1.3 Research Gaps and Thesis Objectives

The initial goal of this thesis is to study the Damariscotta River estuary (DRE) located in Maine with a three-dimensional analytical model derived as in Ensing et al. (2015). Studies of this estuary, primarily observational, are limited, particularly spatially [9, 8, 7]. There is a lack of understanding of the driving forces of flow within the DRE and sediment transport within the estuary. This thesis applies an analytical model focusing on the tidal flow within the entire DRE to gain insight into the dynamics within the estuary.

The Damariscotta River estuary is a drowned river valley estuary that is tidally-dominated and weakly-stratified. It is short and narrow with a length of 30 km and maximum width of 975 m at the mouth. The DRE is convergent, with width of 45 m at the head, and relatively shallow, with average depth of 10 m. The tides are semi-diurnal dominated, and the tidal range varies from 2.2 to 3.6 m during neap and spring tides [7]. Aquaculture within the estuary thrives playing a vital role in the local economy.

There are several objectives which are used to achieve the initial goal. The first objective of this thesis is to study tidal wave propagation along the estuary, investigating along-channel variations in water level and velocity. The second objective is to gain understanding of three-dimensional tidal current velocity variations within the estuary. The rest of this thesis is as follows. Chapter two describes a detailed derivation of the model. Chapter three presents the results of the model and a discussion of their implications.

CHAPTER 2

METHODS

2.1 Model Derivation

2.1.1 Equations and Variables

This section contains the equations and variables that will be used to develop the model. First, we will define all variables and parameters. Along-channel distance is measured along the x -axis, across-channel is measured along the y -axis, and depth is measured along the z -axis. Along-channel, across-channel, and vertical velocities are given by u , v , and w , respectively. Density is defined by ρ . Gravitational acceleration, g , is 9.81 m s^{-2} . Vertical eddy viscosity is defined by A_v . The sea surface height is defined by η . The amplitude, at the seaward end, and angular frequency of the M_2 tidal component are defined by A_{M_2} and ω , respectively. The Coriolis parameter is defined by f and is calculated as $f = 2\Omega \sin \phi$, where ϕ is latitude of the estuary and $\Omega = 7.2921 \times 10^{-5} \text{ rad s}^{-1}$ is the rotation rate of the Earth.

The estuary was modeled as in [4], shown in Fig.2.1. The dimensions of the estuary are defined by the following: length from mouth to head is L_c , width at the mouth is B , and maximum depth is h_{max} . However, estuary width varies along-channel. So we define estuary width more generally as b , which is a function of x :

$$b(x) = B e^{\frac{-x}{L_b}}, \quad (2.1)$$

where L_b is the e -folding length or the distance along the estuary it takes for the width to decrease by a factor of e . Known values of important physical parameters, specific to the Damariscotta River Estuary, are given in Table 1.

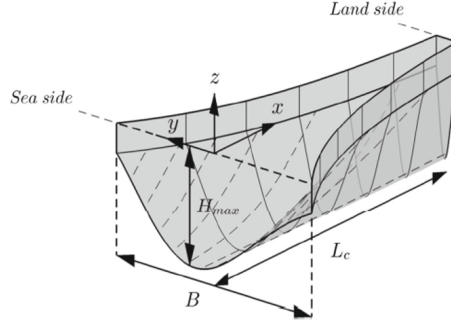


Figure 2.1. Model estuary schematic [4].

Known values of important physical parameters, specific to the Damariscotta River Estuary, are given in Table 1.

Parameter	Symbol	Value
Maximum water depth	h_{max}	45 m
Average water depth	\bar{h}	10 m
Width at mouth	B	963 m
Width at head	b_{head}	45 m
Length	L_c	30.6 km
e -folding length	L_b	58 km
Frictionless M_2 tidal wavelength divided by 2π	L_t	69.6 km
Amplitude of M_2 tidal elevation at the seaward end	A_{M_2}	1.50 m
Angular frequency of the M_2 tidal component	ω	$1.41 \times 10^{-4} \text{ s}^{-1}$
Gravitational acceleration	g	9.81 m s^{-2}
Coriolis parameter	f	$1.01 \times 10^{-4} \text{ s}^{-1}$
Vertical eddy viscosity	A_v	$10^{-2.5} \text{ m}^2 \text{ s}^{-1}$
Reference density	ρ_0	1024 kg m^{-3}
Reference salinity	s_{ref}	31.8 psu
Slip parameter at reference depth	S_{ref}	10^5 m s^{-2}

Table 2.1. Parameter values for the Damariscotta River estuary

Next, we present the equations and boundary conditions used to derive the model. The horizontal Reynolds averaged Navier-Stokes equations in the shallow water limit are given by Eqs. (2.2) and (2.3)). The first term on the left hand side (LHS) is the local acceleration, which describes changes in velocity with time. The next three terms are the advective accelerations, or changes in velocity with space. The last term of the LHS represents the Coriolis acceleration, which is due to the rotation of the earth. On the right hand side (RHS), the first term is the barotropic pressure gradient due to spatial differences in water level. The next term is the baroclinic pressure gradient due to spatial differences in density. The last term is the friction (stress divergence) with depth varying vertical eddy viscosity.

$$\frac{\partial u}{\partial t} + u \frac{\partial u}{\partial x} + v \frac{\partial u}{\partial y} + w \frac{\partial u}{\partial z} - fv = -g \frac{\partial \eta}{\partial x} + \frac{g}{\rho_w} \int_{-h}^{\eta} \frac{\partial \rho}{\partial x} dz + \frac{\partial}{\partial z} A_v \frac{\partial u}{\partial z} \quad (2.2)$$

$$\frac{\partial v}{\partial t} + u \frac{\partial v}{\partial x} + v \frac{\partial v}{\partial y} + w \frac{\partial v}{\partial z} + fu = -g \frac{\partial \eta}{\partial y} + \frac{g}{\rho_w} \int_{-h}^{\eta} \frac{\partial \rho}{\partial y} dz + \frac{\partial}{\partial z} A_v \frac{\partial v}{\partial z} \quad (2.3)$$

The continuity equation, Eq. (2.4), is the conservation of mass or that there is no loss of water in the estuary.

$$\frac{\partial u}{\partial x} + \frac{\partial v}{\partial y} + \frac{\partial w}{\partial z} = 0 \quad (2.4)$$

We have the following boundary conditions. At the surface, $z = \eta$, we have no stress:

$$A_v \frac{\partial u}{\partial z} = A_v \frac{\partial v}{\partial z} = 0, \quad (2.5)$$

and the kinematic free surface boundary condition (i.e. the vertical movement of fluid particles is with the movement of the free surface):

$$w = \frac{\partial \eta}{\partial t} + u \frac{\partial \eta}{\partial x} + v \frac{\partial \eta}{\partial y}. \quad (2.6)$$

At the bottom boundary, $z = -h$, we have partial slip, expressed by three equations

$$A_v \frac{\partial u}{\partial z} = Su, \quad (2.7)$$

$$A_v \frac{\partial v}{\partial z} = Sv, \quad (2.8)$$

where S is the slip parameter, and

$$w = -v \frac{\partial h}{\partial y}, \quad (2.9)$$

where $h = f(y)$ is the depth, which will be described later.

The sides of the estuary, $y = \pm \frac{b}{2}$, are assumed to be impermeable, expressed by

$$\int_{-h}^{\eta} v dz = \pm \frac{1}{2} \frac{\partial b}{\partial x} \int_{-h}^{\eta} u dz. \quad (2.10)$$

At the mouth, $x = 0$, the water motion is forced solely to the semi-diurnal tide, with a period of 12.42 h, mathematically expressed as

$$\eta = A_{M_2} \cos(\omega t), \quad (2.11)$$

where A_{M_2} is the amplitude at the seaward end and ω is the angular frequency of the M_2 tidal component. At the head of the estuary, $x = L_c$, we assume that there is no transport through the upstream boundary:

$$\int_{-h}^{\eta} u dz = 0. \quad (2.12)$$

The density balance is

$$\frac{\partial \rho}{\partial t} + u \frac{\partial \rho}{\partial x} + v \frac{\partial \rho}{\partial y} + w \frac{\partial \rho}{\partial z} = \frac{K_v}{2} \frac{\partial^2 \rho}{\partial z^2}, \quad (2.13)$$

where K_v is the vertical eddy diffusion coefficient. Note that K_v is constant with respect to depth. The density balance states that the local and advective changes in density are balanced by mixing. We assume no vertical variation in density from the surface ($z = \eta$) to the bottom ($z = -h$) of the estuary, written by

$$\frac{\partial \rho}{\partial z} = 0. \quad (2.14)$$

2.1.1.1 Integrated Continuity Equation

In order to solve the dynamical system above, the integrated continuity equation, over depth and across-channel, was also needed. To integrate the continuity equation, Eq. (2.4),

we applied the shallow water assumption, which allows integration over depth, and several of the boundary conditions: Eq. (2.6), Eq. (2.9), and Eq. (2.10). We first integrate over depth from the bottom, $-h$, to the free surface, η :

$$\int_{-h}^{\eta} \left(\frac{\partial u}{\partial x} + \frac{\partial v}{\partial y} + \frac{\partial w}{\partial z} = 0 \right) dz,$$

which becomes

$$\int_{-h}^{\eta} \frac{\partial u}{\partial x} dz + \int_{-h}^{\eta} \frac{\partial v}{\partial y} dz + w|_{z=\eta} - w|_{z=-h} = 0. \quad (2.15)$$

. We apply the kinematic free surface, Eq. (2.6), and partial slip, Eq. (2.8), boundary conditions to Eq. (2.15):

$$\int_{-h}^{\eta} \frac{\partial u}{\partial x} dz + \int_{-h}^{\eta} \frac{\partial v}{\partial y} dz + \frac{\partial \eta}{\partial t} + u \frac{\partial \eta}{\partial x} + v \frac{\partial \eta}{\partial y} + v \frac{\partial h}{\partial y} = 0. \quad (2.16)$$

Next, we apply the Leibniz Integral Rule to the first two terms of Eq. (2.16):

$$\begin{aligned} \frac{\partial}{\partial x} \int_{-h}^{\eta} u dz - u \frac{\partial \eta}{\partial x} + u \frac{\partial(-h)}{\partial x} + \frac{\partial}{\partial y} \int_{-h}^{\eta} v dz - v \frac{\partial \eta}{\partial y} + v \frac{\partial(-h)}{\partial y} \\ + \frac{\partial \eta}{\partial t} + u \frac{\partial \eta}{\partial x} + v \frac{\partial \eta}{\partial y} + v \frac{\partial h}{\partial y} = 0. \end{aligned} \quad (2.17)$$

Note that h is a function of y so $\frac{\partial h}{\partial x} = 0$. After canceling terms, we obtain

$$\frac{\partial}{\partial x} \int_{-h}^{\eta} u dz + \frac{\partial}{\partial y} \int_{-h}^{\eta} v dz + \frac{\partial \eta}{\partial t} = 0. \quad (2.18)$$

We move the first two terms over to the RHS and integrate across-channel, from $-\frac{b}{2}$ to $\frac{b}{2}$, resulting in the following:

$$\int_{-\frac{b}{2}}^{\frac{b}{2}} \frac{\partial \eta}{\partial t} dy = - \int_{-\frac{b}{2}}^{\frac{b}{2}} \frac{\partial}{\partial x} \int_{-h}^{\eta} u dz dy - \int_{-\frac{b}{2}}^{\frac{b}{2}} \frac{\partial}{\partial y} \int_{-h}^{\eta} v dz dy. \quad (2.19)$$

Eq. (2.19) can be further evaluated as

$$b \frac{\partial \eta}{\partial t} = - \int_{-\frac{b}{2}}^{\frac{b}{2}} \frac{\partial}{\partial x} \int_{-h}^{\eta} u dz dy - \int_{-h}^{\eta} v dz \Big|_{y=\frac{b}{2}} + \int_{-h}^{\eta} v dz \Big|_{y=-\frac{b}{2}}. \quad (2.20)$$

We apply Eq. (2.10) to obtain:

$$b \frac{\partial \eta}{\partial t} = - \int_{-\frac{b}{2}}^{\frac{b}{2}} \frac{\partial}{\partial x} \int_{-h}^{\eta} u \, dz \, dy - \frac{1}{2} \frac{\partial b}{\partial x} \int_{-h}^{\eta} u \, dz - \frac{1}{2} \frac{\partial b}{\partial x} \int_{-h}^{\eta} u \, dz, \quad (2.21)$$

which simplifies to

$$b \frac{\partial \eta}{\partial t} = - \int_{-\frac{b}{2}}^{\frac{b}{2}} \frac{\partial}{\partial x} \int_{-h}^{\eta} u \, dz \, dy - \frac{\partial b}{\partial x} \int_{-h}^{\eta} u \, dz. \quad (2.22)$$

We apply the Leibniz Integral rule again:

$$b \frac{\partial \eta}{\partial t} = - \frac{\partial}{\partial x} \int_{-\frac{b}{2}}^{\frac{b}{2}} \int_{-h}^{\eta} u \, dz \, dy + \frac{\partial(\frac{b}{2})}{\partial x} \int_{-h}^{\eta} u \, dz - \frac{\partial(-\frac{b}{2})}{\partial x} \int_{-h}^{\eta} u \, dz - \frac{\partial b}{\partial x} \int_{-h}^{\eta} u \, dz. \quad (2.23)$$

Then, we simplify Eq. (2.23) to

$$b \frac{\partial \eta}{\partial t} = - \frac{\partial}{\partial x} \int_{-\frac{b}{2}}^{\frac{b}{2}} \int_{-h}^{\eta} u \, dz \, dy + \frac{1}{2} \frac{\partial b}{\partial x} \int_{-h}^{\eta} u \, dz + \frac{1}{2} \frac{\partial b}{\partial x} \int_{-h}^{\eta} u \, dz - \frac{\partial b}{\partial x} \int_{-h}^{\eta} u \, dz. \quad (2.24)$$

After canceling terms, we have the integrated continuity equation, which completes the system and allows solution for water level, η , given by

$$b \frac{\partial \eta}{\partial t} = - \frac{\partial}{\partial x} \int_{-\frac{b}{2}}^{\frac{b}{2}} \int_{-h}^{\eta} u \, dz \, dy. \quad (2.25)$$

2.1.2 Non-dimensionalization

In order to perform perturbation analysis, we non-dimensionalize all equations and boundary conditions. The following scaling, where $'$ denotes a non-dimensional variable, will be applied in this section:

$$\begin{aligned} t &= \frac{t'}{\omega}, & f &= \omega f', & x &= L_c x', & y &= B y', & b &= B b', & z &= h_{max} z', & h &= h_{max} h', \\ \eta &= A_{M_2} \eta', & u &= U u', & v &= V v', & w &= W w', & \rho &= \Delta \rho p', & s &= \Delta s s', \\ A_v &= \frac{\omega h_{max}^2 A'_v}{2}, & K_v &= \frac{\omega h_{max}^2 K'_v}{2} & S &= \frac{\omega h_{max} S'}{2} \end{aligned} \quad (2.26)$$

First, we plug the parameters in Eq. (2.26) into the continuity equation, Eq. (2.4), and momentum equations, Eqs. (2.2) and (2.3), to obtain:

$$\frac{U\partial u'}{L_c\partial x'} + \frac{V\partial v'}{B\partial y'} + \frac{W\partial w'}{h_{max}\partial z'} = 0 \quad (2.27)$$

$$\begin{aligned} \omega U \frac{\partial u'}{\partial t'} + \frac{U^2 u'}{L_c} \frac{\partial u'}{\partial x'} + \frac{V U v'}{B} \frac{\partial u'}{\partial y'} + \frac{W U w'}{h_{max}} \frac{\partial u'}{\partial z'} - \omega V f' v' = \\ - \frac{g A_{M_2}}{L_c} \frac{\partial \eta'}{\partial x'} + \frac{g h_{max} \Delta \rho}{\rho_w L_c} \int_{-h'}^{\epsilon \eta'} \eta \frac{\partial \rho'}{\partial x'} dz' + \frac{U \omega A'_v h_{max}^2}{2 h_{max}^2} \frac{\partial^2 u'}{\partial z'^2} \end{aligned} \quad (2.28)$$

$$\begin{aligned} \omega V \frac{\partial v'}{\partial t'} + \frac{U V u'}{L_c} \frac{\partial v'}{\partial x'} + \frac{V^2 v'}{B} \frac{\partial v'}{\partial y'} + \frac{W V w'}{h_{max}} \frac{\partial v'}{\partial z'} + \omega U f' u' = \\ - \frac{g A_{M_2}}{B} \frac{\partial \eta'}{\partial y'} + \frac{g h_{max} \Delta \rho}{\rho_w B} \int_{-h'}^{\epsilon \eta'} \frac{\partial \rho'}{\partial y'} dz' + \frac{V \omega A'_v h_{max}^2}{2 h_{max}^2} \frac{\partial^2 v'}{\partial z'^2} \end{aligned} \quad (2.29)$$

Multiplying Eq. (2.28) by $\frac{1}{U\omega}$ and Eq. (2.29) by $\frac{1}{V\omega}$, we obtain:

$$\begin{aligned} \frac{\partial u'}{\partial t'} + \frac{U u'}{\omega L_c} \frac{\partial u'}{\partial x'} + \frac{V v'}{\omega B} \frac{\partial u'}{\partial y'} + \frac{W w'}{\omega h_{max}} \frac{\partial u'}{\partial z'} - \frac{V}{U} f' v' = \\ - \frac{g A_{M_2}}{\omega U L_c} \frac{\partial \eta'}{\partial x'} + \frac{g h_{max} \Delta \rho}{\omega U \rho_w L_c} \int_{-h'}^{\epsilon \eta'} \frac{\partial \rho'}{\partial x'} dz' + \frac{A'_v}{2} \frac{\partial^2 u'}{\partial z'^2} \end{aligned} \quad (2.30)$$

$$\begin{aligned} \frac{\partial v'}{\partial t'} + \frac{U u'}{\omega L_c} \frac{\partial v'}{\partial x'} + \frac{V v'}{\omega B} \frac{\partial v'}{\partial y'} + \frac{W w'}{\omega h_{max}} \frac{\partial v'}{\partial z'} + \frac{U}{V} f' u' = \\ - \frac{g A_{M_2}}{\omega V B} \frac{\partial \eta'}{\partial y'} + \frac{g h_{max} \Delta \rho}{\omega V \rho_w B} \int_{-h'}^{\epsilon \eta'} \frac{\partial \rho'}{\partial y'} dz' + \frac{A'_v}{2} \frac{\partial^2 v'}{\partial z'^2} \end{aligned} \quad (2.31)$$

From the continuity equation, it is assumed that $\frac{\partial u}{\partial x} \approx \frac{\partial v}{\partial y} \approx \frac{\partial w}{\partial z}$ [4]. In terms of scaling, we have

$$\frac{U}{L_c} = \frac{V}{B} = \frac{W}{h_{max}}. \quad (2.32)$$

The local change in water level elevation is balanced by the change in the along-channel velocity. This means that $\frac{\partial \eta}{\partial t} \approx h_{max} \frac{\partial u}{\partial x}$ and, therefore, we assume

$$A_{M_2} \omega = \frac{h_{max} U}{L_c}. \quad (2.33)$$

We define the following non-dimensional parameters:

$$\epsilon = \frac{A_{M_2}}{h_{max}}, \quad (2.34)$$

$$\alpha = \frac{B}{L_c}, \quad (2.35)$$

$$\gamma = \frac{\Delta\rho}{\epsilon\alpha\rho_w}, \quad (2.36)$$

$$\mu = \frac{L_c}{L_b}, \quad (2.37)$$

where ϵ is the ratio between the tidal elevation and the water depth, α is the horizontal aspect ratio of the estuary, γ is the density gradient scale, and μ is the width convergence factor [4].

From Eqs. (2.32) and (2.33), we write ϵ as

$$\epsilon = \frac{A_{M_2}}{h_{max}} = \frac{U}{\omega L_c} = \frac{V}{\omega B} = \frac{W}{\omega h_{max}}. \quad (2.38)$$

Using Eq. (2.38), we can rewrite Eq. (2.27) as

$$\epsilon\omega\left(\frac{\partial u'}{\partial x'} + \frac{\partial v'}{\partial y'} + \frac{\partial w'}{\partial z'}\right) = 0. \quad (2.39)$$

Then, if we divide Eq. (2.39) by $\epsilon\omega$, we get the non-dimensional continuity equation:

$$\frac{\partial u'}{\partial x'} + \frac{\partial v'}{\partial y'} + \frac{\partial w'}{\partial z'} = 0. \quad (2.40)$$

We substitute the non-dimensional parameters defined in Eqs. (2.34) - (2.36) to simplify Eqs. (2.30) and (2.31), obtaining

$$\begin{aligned} & \frac{\partial u'}{\partial t'} + \epsilon\left(u'\frac{\partial u'}{\partial x'} + v'\frac{\partial u'}{\partial y'} + w'\frac{\partial u'}{\partial z'}\right) - \alpha f'v' \\ &= -\frac{gh_{max}}{\omega^2 L_c^2} \frac{\partial \eta'}{\partial x'} + \frac{gh_{max}\alpha\gamma\epsilon}{\omega U L_c} \int_{-h'}^{\epsilon\eta'} \frac{\partial \rho'}{\partial x'} dz' + \frac{A'_v}{2} \frac{\partial^2 u'}{\partial z'^2} \end{aligned} \quad (2.41)$$

and

$$\begin{aligned} & \frac{\partial v'}{\partial t'} + \epsilon\left(u'\frac{\partial v'}{\partial x'} + v'\frac{\partial v'}{\partial y'} + w'\frac{\partial v'}{\partial z'}\right) + \frac{1}{\alpha} f'u' \\ &= -\frac{gh_{max}}{B^2\omega^2} \frac{\partial \eta'}{\partial y'} + \frac{gh_{max}\epsilon\alpha\gamma}{\omega V B} \int_{-h'}^{\epsilon\eta'} \frac{\partial \rho'}{\partial y'} dz' + \frac{A'_v}{2} \frac{\partial^2 v'}{\partial z'^2}. \end{aligned} \quad (2.42)$$

From Eq. (2.38), $\frac{\epsilon}{U} = \frac{1}{\omega L_c}$ and $\frac{\epsilon}{V} = \frac{1}{\omega B}$. Eqs. (2.41) and (2.42) become

$$\begin{aligned} & \frac{\partial u'}{\partial t'} + \epsilon \left(u' \frac{\partial u'}{\partial x'} + v' \frac{\partial u'}{\partial y'} + w' \frac{\partial u'}{\partial z'} \right) - \alpha f' v' \\ &= -\frac{gh_{max}}{\omega^2 L_c^2} \frac{\partial \eta'}{\partial x'} + \frac{gh_{max} \alpha \gamma}{\omega^2 L_c^2} \int_{-h'}^{\epsilon \eta'} \frac{\partial \rho'}{\partial x'} dz' + \frac{A'_v}{2} \frac{\partial^2 u'}{\partial z'^2} \end{aligned} \quad (2.43)$$

and

$$\begin{aligned} & \frac{\partial v'}{\partial t'} + \epsilon \left(u' \frac{\partial v'}{\partial x'} + v' \frac{\partial v'}{\partial y'} + w' \frac{\partial v'}{\partial z'} \right) + \frac{1}{\alpha} f' u' \\ &= -\frac{gh_{max}}{B^2 \omega^2} \frac{\partial \eta'}{\partial y'} + \frac{gh_{max} \alpha \gamma}{\omega^2 B^2} \int_{-h'}^{\epsilon \eta'} \frac{\partial \rho'}{\partial y'} dz' + \frac{A'_v}{2} \frac{\partial v'^2}{\partial z'^2}. \end{aligned} \quad (2.44)$$

Manipulating Eq. (2.35), we substitute $B = L_c \alpha$ into Eq. (2.44) to obtain

$$\begin{aligned} & \frac{\partial v'}{\partial t'} + \epsilon \left(u' \frac{\partial v'}{\partial x'} + v' \frac{\partial v'}{\partial y'} + w' \frac{\partial v'}{\partial z'} \right) + \frac{1}{\alpha} f' u' \\ &= -\frac{gh_{max}}{\alpha^2 L_c^2 \omega^2} \frac{\partial \eta'}{\partial y'} + \frac{gh_{max} \gamma}{\alpha \omega^2 L_c^2} \int_{-h'}^{\epsilon \eta'} \frac{\partial \rho'}{\partial y'} dz' + \frac{A'_v}{2} \frac{\partial^2 v'}{\partial z'^2}. \end{aligned} \quad (2.45)$$

We define L_t , the frictionless M_2 tidal wavelength, as

$$L_t = \sqrt{\frac{gh_{max}}{\omega^2}}. \quad (2.46)$$

We define l to be the channel length relative to the tidal wavelength [4], expressed as

$$l = \frac{L_c}{L_t}. \quad (2.47)$$

Eqs. (2.43) and (2.45) become

$$\frac{\partial u'}{\partial t'} + \epsilon \left(u' \frac{\partial u'}{\partial x'} + v' \frac{\partial u'}{\partial y'} + w' \frac{\partial u'}{\partial z'} \right) - \alpha f' v' = -\frac{1}{l^2} \frac{\partial \eta'}{\partial x'} + \frac{\alpha \gamma}{l^2} \int_{-h'}^{\epsilon \eta'} \frac{\partial \rho'}{\partial x'} dz' + \frac{A'_v}{2} \frac{\partial^2 u'}{\partial z'^2} \quad (2.48)$$

and

$$\frac{\partial v'}{\partial t'} + \epsilon \left(u' \frac{\partial v'}{\partial x'} + v' \frac{\partial v'}{\partial y'} + w' \frac{\partial v'}{\partial z'} \right) + \frac{1}{\alpha} f' u' = -\frac{1}{l^2 \alpha^2} \frac{\partial \eta'}{\partial y'} + \frac{\gamma}{l^2 \alpha} \int_{-h'}^{\epsilon \eta'} \frac{\partial \rho'}{\partial y'} dz' + \frac{A'_v}{2} \frac{\partial^2 v'}{\partial z'^2}. \quad (2.49)$$

Multiplying Eq. (2.49) by α , we have the non-dimensional horizontal momentum equations:

$$\frac{\partial u'}{\partial t'} + \epsilon \left(u' \frac{\partial u'}{\partial x'} + v' \frac{\partial u'}{\partial y'} + w' \frac{\partial u'}{\partial z'} \right) - \alpha f' v' = -\frac{1}{l^2} \frac{\partial \eta'}{\partial x'} + \frac{\alpha \gamma}{l^2} \int_{-h'}^{\epsilon \eta'} \frac{\partial \rho'}{\partial x'} dz' + \frac{A'_v}{2} \frac{\partial^2 u'}{\partial z'^2} \quad (2.50)$$

and

$$\begin{aligned} \alpha \frac{\partial v'}{\partial t'} + \alpha \epsilon \left(u' \frac{\partial v'}{\partial x'} + v' \frac{\partial v'}{\partial y'} + w' \frac{\partial v'}{\partial z'} \right) + f' u' \\ = -\frac{1}{l^2 \alpha} \frac{\partial \eta'}{\partial y'} + \frac{\gamma}{l^2} \int_{-h'}^{\epsilon \eta'} \frac{\partial \rho'}{\partial y'} dz' + \frac{\alpha A'_v}{2} \frac{\partial^2 v'}{\partial z'^2}. \end{aligned} \quad (2.51)$$

The non-dimensional width equation, from Eq. (2.1), is

$$b'(x') = e^{-\mu x'}. \quad (2.52)$$

Next, we apply the scaling in Eq. (2.26) to the boundary conditions, Eqs. (2.5) - (2.12).

At $z' = \epsilon \eta'$, the stress-free surface boundary condition, Eq. (2.5), becomes

$$\frac{A'_v \omega h_{max}^2 U}{2h_{max}} \frac{\partial u'}{\partial z'} = \frac{A'_v \omega h_{max}^2 V}{2h_{max}} \frac{\partial v'}{\partial z'}, \quad (2.53)$$

which is simplified as

$$U \frac{\partial u'}{\partial z'} = V \frac{\partial v'}{\partial z'}. \quad (2.54)$$

Recall from Eqs. (2.32) and (2.35) that $\alpha = \frac{V}{U}$, so Eq. (2.54) becomes

$$\frac{\partial u'}{\partial z'} = \alpha \frac{\partial v'}{\partial z'}. \quad (2.55)$$

After substituting Eq. (2.26), Eq. (2.6), the non-dimensional kinematic free-surface boundary condition at $z' = \epsilon \eta'$, is

$$W w' = A_{M_2} \omega \frac{\partial \eta'}{\partial t'}. \quad (2.56)$$

From Eqs. (2.32) and (2.33), $W = A_{M_2} \omega$. Thus, we simplify Eq. (2.56) as

$$w' = \frac{\partial \eta'}{\partial t'}. \quad (2.57)$$

We non-dimensionalize Eqs (2.7) - (2.8), partial slip at the bottom boundary ($z' = -h'$), as the following:

$$\frac{A'_v \omega h_{max}^2 U}{2h_{max}} \frac{\partial u'}{\partial z'} = \frac{\omega h_{max}}{2} U S' u',$$

which is simplified to

$$A'_v \frac{\partial u'}{\partial z'} = S' u', \quad (2.58)$$

and

$$\frac{A'_v \omega h_{max}^2 V}{2h_{max}} \frac{\partial v'}{\partial z'} = \frac{\omega h_{max}}{2} V S' v',$$

which is simplified to

$$A'_v \frac{\partial v'}{\partial z'} = S' v'. \quad (2.59)$$

Eq. (2.9) is non-dimensionalized as

$$W w' = - \frac{V h_{max}}{B} v' \frac{\partial h'}{\partial y'}, \quad (2.60)$$

which is simplified using Eqs. (2.32) and (2.33) to

$$w' = - v' \frac{\partial h'}{\partial y'}. \quad (2.61)$$

The sides of the estuary (at $y' = \pm \frac{b'}{2}$) are impermeable, expressed by Eq. (2.10). Its non-dimensional form is

$$V h_{max} \int_{-h'}^{\epsilon \eta'} v' dz' = \pm \frac{B U h_{max}}{2 L_c} \frac{\partial b'}{\partial x'} \int_{-h'}^{\epsilon \eta'} u' dz'.$$

From Eq. (2.32), this is simplified to

$$\int_{-h'}^{\epsilon \eta'} v' dz' = \pm \frac{1}{2} \frac{\partial b'}{\partial x'} \int_{-h'}^{\epsilon \eta'} u' dz'. \quad (2.62)$$

We substitute the partial derivative of the non-dimensional estuary width, Eq. (2.52), with respect to x to get

$$\int_{-h'}^{\epsilon \eta'} v' dz' = \pm \frac{\mu}{2} e^{-\mu x'} \int_{-h'}^{\epsilon \eta'} u' dz'. \quad (2.63)$$

At the mouth of the estuary ($x' = 0$), the water motion is forced by the M_2 semi-diurnal tide, expressed by Eq. (2.11). Its non-dimensional form is given by

$$\eta' = \cos t'. \quad (2.64)$$

At the head of the estuary ($x' = l$) (recall Eq. (2.47)), there is no along-channel transport, expressed by Eq. (2.12). Its non-dimensional form is

$$\int_{-h'}^{\epsilon\eta'} u' dz' = 0. \quad (2.65)$$

Lastly, we non-dimensionalize the integrated continuity equation, Eq. (2.25), and the density balance, Eq. (2.13). The integrated continuity equation becomes

$$\omega B A_{M_2} b' \frac{\partial \eta'}{\partial t'} = - \frac{1}{L_c} \frac{\partial}{\partial x'} \int_{-\frac{Bb'}{2}}^{\frac{Bb'}{2}} \int_{-h_{max}h'}^{A_{M_2}\eta'} U h_{max} B u' dz' dy', \quad (2.66)$$

which is simplified to

$$\omega A_{M_2} b' \frac{\partial \eta'}{\partial t'} = - \frac{U h_{max}}{L_c} \frac{\partial}{\partial x'} \int_{-\frac{b'}{2}}^{\frac{b'}{2}} \int_{-h'}^{\epsilon\eta'} u' dz' dy'. \quad (2.67)$$

Using Eq. (2.32) to cancel the constants, we have the non-dimensional integrated continuity equation:

$$b' \frac{\partial \eta'}{\partial t'} = - \frac{\partial}{\partial x'} \int_{-\frac{b'}{2}}^{\frac{b'}{2}} \int_{-h'}^{\epsilon\eta'} u' dz' dy'. \quad (2.68)$$

The density balance, Eq. (2.13), becomes

$$\Delta\rho\omega \frac{\partial \rho'}{\partial t'} + \frac{U\Delta\rho}{L_c} u' \frac{\partial \rho'}{\partial x'} + \frac{V\Delta\rho}{B} v' \frac{\partial \rho'}{\partial y'} + \frac{W\Delta\rho}{h_{max}} w' \frac{\partial \rho'}{\partial z'} = \frac{K_v\Delta\rho}{h_{max}^2} \frac{\partial^2 \rho'}{\partial z'^2}. \quad (2.69)$$

Note that this is not yet non-dimensional. Multiplying Eq. (2.69) by $\frac{1}{\Delta\rho\omega}$, we obtain

$$\frac{\partial \rho'}{\partial t'} + \epsilon \left(u' \frac{\partial \rho'}{\partial x'} + v' \frac{\partial \rho'}{\partial y'} + w' \frac{\partial \rho'}{\partial z'} \right) = \frac{K_v}{\omega h_{max}^2} \frac{\partial^2 \rho'}{\partial z'^2}. \quad (2.70)$$

Substituting the non-dimensional form of the vertical eddy diffusion coefficient, K_v , we obtain the non-dimensional density balance

$$\frac{\partial \rho'}{\partial t'} + \epsilon \left(u' \frac{\partial \rho'}{\partial x'} + v' \frac{\partial \rho'}{\partial y'} + w' \frac{\partial \rho'}{\partial z} \right) = \frac{K'_v}{2} \frac{\partial^2 \rho'}{\partial z'^2}. \quad (2.71)$$

The non-dimensional density boundary condition, no vertical density change at the mouth and head of the estuary, is

$$\frac{\partial \rho'}{\partial z'} = 0. \quad (2.72)$$

2.1.3 Perturbation Expansion

In order to analyze the system and determine the terms that are important to estuary flow, we construct a perturbation series in ϵ , which is a measure of the non-linearity of the system, of the form:

$$\Psi = \Psi_0 + \epsilon \Psi_1 + \epsilon^2 \Psi_2 + \dots, \quad (2.73)$$

where Ψ represents the each of the non-dimensional variables u' , v' , w' , η' , and ρ' .

We then plug Eq. (2.73) into all equations and boundary conditions and collect terms of the same order. We are only interested in the zero- and first- order terms, because the zero- and first- order solutions represent the tidal flow and the residual flow, respectively, in the estuary. Therefore, we discard terms of order two or greater, and, in most cases, only substitute $\Psi = \Psi_0 + \epsilon \Psi_1$. Using the values in Table 1, we determine that $O(\epsilon) = 0.1$, $O(\alpha) \approx O(\epsilon)$, $O(\gamma) = 1$ (recall Eqs.(2.34), (2.35), and (2.36)). Although l is smaller, we assume $O(l) = 1$ which is more representative of a longer estuary. All variables are non-dimensional so, for simplicity of notation, we drop the apostrophes. We drop constants equal to 1.

The horizontal momentum equations, Eqs. (2.50) and (2.51), are expanded as

$$\begin{aligned} \frac{\partial u_0}{\partial t} + \epsilon \frac{\partial u_1}{\partial t} + \epsilon \left(u_0 \frac{\partial u_0}{\partial x} + v_0 \frac{\partial u_0}{\partial y} + w_0 \frac{\partial u_0}{\partial z} \right) - \alpha f(v_0 + \epsilon v_1) = \\ - \left(\frac{\partial \eta_0}{\partial x} - \epsilon \frac{\partial \eta_1}{\partial x} \right) + \alpha \int_{-h}^{\epsilon \eta} \left(\frac{\partial \rho_0}{\partial x} + \epsilon \frac{\partial \rho_1}{\partial x} \right) dz + \frac{A_v}{2} \frac{\partial}{\partial z} \left(\frac{\partial u_0}{\partial z} + \epsilon \frac{\partial u_1}{\partial z} \right) \end{aligned} \quad (2.74)$$

and

$$\begin{aligned}
& \alpha \left(\frac{\partial v_0}{\partial t} + \epsilon \frac{\partial v_1}{\partial t} \right) + \alpha \epsilon \left(u_0 \frac{\partial v_0}{\partial x} + v_0 \frac{\partial v_0}{\partial y} + w_0 \frac{\partial v_0}{\partial z} \right) + f(u_0 + \epsilon u_1) \\
&= -\frac{1}{\alpha} \left(\frac{\partial \eta_0}{\partial y} + \epsilon \frac{\partial \eta_1}{\partial y} + \epsilon^2 \frac{\partial \eta_2}{\partial y} \right) + \int_{-h}^{\epsilon \eta} \left(\frac{\partial \rho_0}{\partial y} + \epsilon \frac{\partial \rho_1}{\partial y} + \epsilon^2 \frac{\partial \rho_2}{\partial y} \right) dz \\
& \qquad \qquad \qquad + \frac{\alpha A_v}{2} \left(\frac{\partial^2 v_0}{\partial z^2} + \epsilon \frac{\partial^2 v_1}{\partial z^2} \right).
\end{aligned} \tag{2.75}$$

The continuity equation, Eq. (2.40), is expanded as

$$\frac{\partial u_0}{\partial x} + \frac{\partial v_0}{\partial y} + \frac{\partial w_0}{\partial z} + \epsilon \left(\frac{\partial u_1}{\partial x} + \frac{\partial v_1}{\partial y} + \frac{\partial w_1}{\partial z} \right) = 0. \tag{2.76}$$

The integrated continuity equation, Eq. (2.68), is expanded as

$$b \left(\frac{\partial \eta_0}{\partial t} + \epsilon \frac{\partial \eta_1}{\partial t} \right) = - \frac{\partial}{\partial x} \int_{-\frac{b}{2}}^{\frac{b}{2}} \int_{-h}^{\epsilon \eta} \left(u_0 + \epsilon u_1 \right) dz dy. \tag{2.77}$$

The density balance, Eq. (2.71) and the density boundary condition, Eq. (2.72), are expanded as

$$\frac{1}{\epsilon} \left(\frac{\partial \rho_0}{\partial t} + \epsilon \frac{\partial \rho_1}{\partial t} \right) + u_0 \frac{\partial \rho_0}{\partial x} + v_0 \frac{\partial \rho_0}{\partial y} + w_0 \frac{\partial \rho_0}{\partial z} = \frac{K_v}{2\epsilon} \left(\frac{\partial^2 \rho_0}{\partial z^2} + \epsilon \frac{\partial^2 \rho_1}{\partial z^2} \right) \tag{2.78}$$

$$\frac{\partial \rho_0}{\partial z} + \epsilon \frac{\partial \rho_1}{\partial z} = 0. \tag{2.79}$$

Note that ρ_0 is a function solely of x so we drop terms to obtain

$$\frac{\partial \rho_1}{\partial t} + u_0 \frac{\partial \rho_0}{\partial x} = \frac{K_v}{2} \frac{\partial^2 \rho_1}{\partial z^2} \tag{2.80}$$

$$\frac{\partial \rho_1}{\partial z} = 0. \tag{2.81}$$

The no-stress surface boundary condition, Eq. (2.55), is expanded as

$$\frac{\partial u_0}{\partial z} + \epsilon \frac{\partial u_1}{\partial z} = \alpha \left(\frac{\partial v_0}{\partial z} + \epsilon \frac{\partial v_1}{\partial z} \right). \tag{2.82}$$

The kinematic free surface boundary condition, Eq. (2.57), is expanded as

$$w_0 + \epsilon w_1 = \frac{\partial \eta_0}{\partial t} + \epsilon \frac{\partial \eta_1}{\partial t}. \tag{2.83}$$

The partial slip boundary condition (Eqs. (??), (2.59), and (2.61)) is expanded as

$$\frac{A_v}{2} \left(\frac{\partial u_0}{\partial z} + \epsilon \frac{\partial u_1}{\partial z} \right) = S u_0 + \epsilon S u_1, \quad (2.84)$$

$$\frac{A_v}{2} \left(\frac{\partial v_0}{\partial z} + \epsilon \frac{\partial v_1}{\partial z} \right) = S v_0 + \epsilon S v_1, \quad (2.85)$$

and

$$w_0 + \epsilon w_1 = - \left(v_0 + \epsilon v_1 \right) \frac{\partial h}{\partial y}. \quad (2.86)$$

The impermeable side boundary condition, Eq. (2.63), is expanded as

$$\int_{-h}^{\epsilon \eta} \left(v_0 + \epsilon v_1 \right) dz = \pm \frac{\mu}{2} e^{-\mu x} \int_{-h}^{\epsilon \eta} \left(u_0 + \epsilon u_1 \right) dz. \quad (2.87)$$

The boundary condition at the mouth of the estuary, Eq. (2.64), is expanded as

$$\eta_0 + \epsilon \eta_1 = \cos t. \quad (2.88)$$

The boundary condition at the head of the estuary, Eq. (2.65), is expanded as

$$\int_{-h}^{\epsilon \eta} \left(u_0 + \epsilon u_1 \right) dz = 0. \quad (2.89)$$

2.1.4 Zero-order Problem and Solution

For simplification, we consider constant vertical eddy viscosity, A_v , with respect to depth. The zero-order (or lowest-order) problem follows with equations given in Eqs.

(2.90) - (2.94) and boundary conditions given in Eqs. (2.95) - (2.103):

$$\frac{\partial u_0}{\partial t} = - \frac{\partial \eta_0}{\partial x} + \frac{A_v}{2} \frac{\partial^2 u_0}{\partial z^2} \quad (2.90)$$

$$f u_0 = - \frac{1}{\alpha} \left(\frac{\partial \eta_0}{\partial y} + \epsilon \frac{\partial \eta_1}{\partial y} \right) + \int_{-h}^0 \frac{\partial \rho_0}{\partial y} dz \quad (2.91)$$

$$\frac{\partial u_0}{\partial x} + \frac{\partial v_0}{\partial y} + \frac{\partial w_0}{\partial z} = 0 \quad (2.92)$$

$$b \frac{\partial \eta_0}{\partial t} = - \frac{\partial}{\partial x} \int_{-\frac{b}{2}}^0 \int_{-h}^0 u_0 dz dy \quad (2.93)$$

$$\frac{\partial \rho_1}{\partial t} + u_0 \frac{\partial \rho_0}{\partial x} = \frac{K_v}{2} \frac{\partial^2 \rho_1}{\partial z^2} \quad (2.94)$$

$$\frac{\partial \rho_1}{\partial z} = 0 \quad (\text{density boundary condition}) \quad (2.95)$$

$$\frac{\partial u_0}{\partial z} = 0 \quad (\text{no stress surface}) \quad (2.96)$$

$$w_0 = \frac{\partial \eta_0}{\partial t} \quad (\text{kinematic free surface}) \quad (2.97)$$

$$\frac{A_v}{2} \frac{\partial u_0}{\partial z} = S u_0 \quad (\text{partial slip}) \quad (2.98)$$

$$\frac{A_v}{2} \frac{\partial v_0}{\partial z} = S v_0 \quad (\text{partial slip}) \quad (2.99)$$

$$w_0 = -v_0 \frac{\partial h}{\partial y} \quad (\text{partial slip}) \quad (2.100)$$

$$\int_{-h}^0 v_0 dz = \pm \frac{\mu}{2} e^{-\mu x} \int_{-h}^0 u_0 dz \quad (\text{impermeable sides}) \quad (2.101)$$

$$\eta_0 = \cos t \quad (\text{estuary mouth}) \quad (2.102)$$

$$\int_{-h}^0 u_0 dz = 0 \quad (\text{estuary head}) \quad (2.103)$$

Note that v_0 is not present in the zero order across channel momentum equation. Thus, we will also examine the first order. Then, we will solve a linear combination of the zero and first order equations. The first order terms are given by

$$\alpha \frac{\partial v_0}{\partial t} + \epsilon f u_1 = -\frac{\epsilon^2}{\alpha} \frac{\partial \eta_2}{\partial y} + \epsilon \int_{-h}^0 \frac{\partial \rho_1}{\partial y} dz + \frac{\alpha A_v}{2} \frac{\partial^2 v_0}{\partial z^2}. \quad (2.104)$$

We assume that along-channel velocity, u , is a combination of the depth-averaged and depth-varying components, denoted with the subscripts da and dv , respectively, and $\frac{u_{da}}{u_{dv}} = O(\epsilon)$. Thus, we have $u_0 = u_{0,da} + \epsilon u_{0,dv}$. Combining the zero and first order lateral momentum terms, we have

$$\begin{aligned} \alpha \frac{\partial v_0}{\partial t} + f u_{0,da} + \epsilon f u_{0,dv} &= -\frac{1}{\alpha} \left(\frac{\partial \eta_0}{\partial y} + \epsilon \frac{\partial \eta_1}{\partial y} + \epsilon^2 \frac{\partial \eta_2}{\partial y} \right) \\ &+ \int_{-h}^0 \left(\frac{\partial \rho_0}{\partial y} + \epsilon \frac{\partial \rho_1}{\partial y} \right) dz + \frac{\alpha A_v}{2} \frac{\partial^2 v_0}{\partial z^2}. \end{aligned} \quad (2.105)$$

Recall, surface elevation and density does not vary across channel in the zero order, due to the basin being narrow and well-mixed. Let $\eta' = \eta_1 + \epsilon\eta_2$ be the higher order surface elevation effects, which will be solved for as a single variable. We have

$$\alpha \frac{\partial v_0}{\partial t} + f u_0 = -\frac{\epsilon}{\alpha} \frac{\partial \eta'}{\partial y} + \int_{-h}^0 \epsilon \frac{\partial \rho_1}{\partial y} dz + \frac{\alpha A_v}{2} \frac{\partial^2 v_0}{\partial z^2}. \quad (2.106)$$

For periodic solutions, we substitute

$$(u_0, v_0, w_0, \eta_0, \eta_1, \rho_1) = \text{Re}((U_0, V_0, W_0, N_0, N_1, \hat{\rho}_1) e^{-it}) \quad (2.107)$$

into all equations and boundary conditions. Note that U_0, V_0, W_0 , and N_0 are the complex amplitudes, or magnitude, of the horizontal and vertical velocities and the sea surface elevation, respectively. The governing equations, (2.90) - (2.94), become

$$iU_0 = -\frac{\partial N_0}{\partial x} + \frac{A_v}{2} \frac{\partial}{\partial z} \frac{\partial U_0}{\partial z} \quad (2.108)$$

$$-i\alpha V_0 + fU_0 = -\frac{\epsilon}{\alpha} \frac{\partial N'}{\partial y} + \epsilon \int_{-h}^0 \frac{\partial \hat{\rho}_1}{\partial y} dz + \frac{\alpha A_v}{2} \frac{\partial^2 V_0}{\partial z^2} \quad (2.109)$$

$$\frac{\partial U_0}{\partial x} + \frac{\partial V_0}{\partial y} + \frac{\partial W_0}{\partial z} = 0 \quad (2.110)$$

$$-ibN_0 = -\frac{\partial}{\partial x} \int_{-\frac{b}{2}}^{\frac{b}{2}} \int_{-h}^0 U_0 dz dy \quad (2.111)$$

$$-i\hat{\rho}_1 + U_0 \frac{d\rho_0}{dx} = \frac{K_v}{2} \frac{\partial^2 \hat{\rho}_1}{\partial z^2} \quad (2.112)$$

The boundary conditions, (2.95) - (2.103), become

$$\frac{\partial \hat{\rho}_1}{\partial z} = 0 \quad (\text{density boundary condition}) \quad (2.113)$$

$$\frac{\partial U_0}{\partial z} = 0 \quad (\text{no stress surface}) \quad (2.114)$$

$$\frac{\partial V_0}{\partial z} = 0 \quad (\text{no stress surface}) \quad (2.115)$$

$$W_0 = -iN_0 \quad (\text{kinematic free surface}) \quad (2.116)$$

$$\frac{A_v}{2} \frac{\partial U_0}{\partial z} = S U_0 \quad (\text{partial slip}) \quad (2.117)$$

$$\frac{A_v}{2} \frac{\partial V_0}{\partial z} = S V_0 \quad (\text{partial slip}) \quad (2.118)$$

$$W_0 = -V_0 \frac{\partial h}{\partial y} \quad (\text{partial slip}) \quad (2.119)$$

$$\int_{-h}^0 V_0 dz = \pm \frac{\mu}{2} e^{-\mu x} \int_{-h}^0 U_0 dz \quad (\text{impermeable sides}) \quad (2.120)$$

$$N_0 = 1 \quad (\text{estuary mouth}) \quad (2.121)$$

$$\int_{-h}^0 U_0 dz = 0 \quad (\text{estuary head}) \quad (2.122)$$

Recall, non-dimensional width, $b(x)$, is given by Eq. (2.52). Depth, $h(y)$, is modeled as a non-dimensional parabolic function of y , given by

$$h(y) = \epsilon + (1 - \epsilon)(1 - y^2). \quad (2.123)$$

We solve the above system for all unknown variables analytically, i.e. on paper.

2.1.4.1 Along-channel Velocity

First, we solve for the along-channel velocity, U_0 , by solving Eq. (2.108). After multiplying by $\frac{2}{A_v}$ and rearranging terms, we have

$$\frac{\partial^2 U_0}{\partial z^2} + \frac{2i}{A_v} U_0 = \frac{2}{A_V} \frac{dN_0}{dx}. \quad (2.124)$$

Let $\Gamma^2 = \frac{-2i}{A_v}$ (Ensing et al., 2016). Then, Eq. (2.124) becomes

$$\frac{\partial^2 U_0}{\partial z^2} - \Gamma^2 U_0 = \frac{2}{A_V} \frac{dN_0}{dx} \quad (2.125)$$

The solution to the homogeneous problem, $\frac{\partial^2 U_0}{\partial z^2} - \Gamma^2 U_0 = 0$, is

$$U_{0,h} = C_1 e^{\Gamma z} + C_2 e^{-\Gamma z}. \quad (2.126)$$

The non-homogeneous, particular, solution is

$$U_{0,nh} = -i \frac{dN_0}{dx}. \quad (2.127)$$

So the total solution is given by

$$U_0 = U_{0,h} + U_{0,nh} = C_1 e^{\Gamma z} + C_2 e^{-\Gamma z} - i \frac{dN_0}{dx}. \quad (2.128)$$

Applying the surface boundary condition, Eq. (2.114), we have that $C_1 = C_2$. The solution then becomes

$$U_0 = C_1 (e^{\Gamma z} + e^{-\Gamma z}) - i \frac{dN_0}{dx}. \quad (2.129)$$

We apply the hyperbolic-trigonometric identity, $\cosh(z) = \frac{e^z + e^{-z}}{2}$, to obtain

$$U_0 = 2C_1 \cosh(\Gamma z) - i \frac{dN_0}{dx}. \quad (2.130)$$

Next, we apply the bottom boundary condition, Eq. (2.117)

$$\frac{A_v}{2} \left(2C_1 \gamma \sinh(-\Gamma h) \right) = S \left(2C_1 \cosh(-\Gamma h) - i \frac{\partial N_0}{\partial x} \right) \quad (2.131)$$

and solve for the constant, C_1 :

$$C_1 = \frac{-i S \frac{dN_0}{dx}}{\Gamma A_v \sinh(-\Gamma h) - 2S \cosh(-\Gamma h)}. \quad (2.132)$$

Factoring $2S$ in the denominator of Eq. (2.132), we obtain

$$C_1 = \frac{-i \frac{\partial N_0}{\partial x}}{2 \left(\frac{\Gamma A_v}{2S} \sinh(-\Gamma h) - \cosh(-\Gamma h) \right)}. \quad (2.133)$$

Substituting $\delta = \frac{2S}{A_v}$ (Ensing et al., 2015) into Eq. (2.132), we have

$$C_1 = \frac{-i \frac{dN_0}{dx}}{2 \left(\frac{\Gamma}{\delta} \sinh(-\Gamma h) - \cosh(-\Gamma h) \right)}. \quad (2.134)$$

So the zero-order solution for the along-channel velocity magnitude is

$$U_0 = i \frac{dN_0}{dx} \left(\frac{-2 \cosh(\Gamma z)}{2 \left(\frac{\Gamma}{\delta} \sinh(-\Gamma h) - \cosh(-\Gamma h) \right)} - 1 \right). \quad (2.135)$$

Since $\cosh(-z) = \cosh(z)$ and $\sinh(-z) = -\sinh(z)$, we have

$$U_0 = i \frac{dN_0}{dx} \left(\frac{-2 \cosh(\Gamma z)}{-2 \left(\frac{\Gamma}{\delta} \sinh(\Gamma h) + \cosh(\Gamma h) \right)} - 1 \right). \quad (2.136)$$

Eq. (2.136) is simplified to give the final solution for U_0 ,

$$U_0 = -i \frac{dN_0}{dx} \left(1 - \frac{\cosh(\Gamma z)}{\cosh(\Gamma h) + \frac{\Gamma}{\delta} \sinh(\Gamma h)} \right). \quad (2.137)$$

2.1.4.2 Water Level

Next, N_0 is solved for by converting the integrated continuity equation, Eq. (2.111), into a homogeneous ordinary differential equation. We first substitute the solution for U_0 into Eq. (2.111).

$$-ibN_0 = i \frac{\partial}{\partial x} \int_{-\frac{b}{2}}^{\frac{b}{2}} \int_{-h}^0 \frac{dN_0}{dx} \left(1 - \frac{\cosh(\Gamma z)}{\cosh(\Gamma h) + \frac{\Gamma}{\delta} \sinh(\Gamma h)} \right) dz dy. \quad (2.138)$$

Eq. (2.138) is simplified to

$$-bN_0 = \frac{\partial}{\partial x} \frac{\partial N_0}{\partial x} \int_{-\frac{b}{2}}^{\frac{b}{2}} \int_{-h}^0 \left(1 - \frac{\cosh(\Gamma z)}{\cosh(\Gamma h) + \frac{\Gamma}{\delta} \sinh(\Gamma h)} \right) dz dy. \quad (2.139)$$

Let

$$p_o = 1 - \frac{\cosh(\Gamma z)}{\cosh(\Gamma h) + \frac{\Gamma}{\delta} \sinh(\Gamma h)}. \quad (2.140)$$

To perform a change of variables, let $y' = \frac{2y}{b}$. Then, Eq. (2.139) becomes

$$-bN_0 = \frac{\partial}{\partial x} \frac{b}{2} \frac{\partial N_0}{\partial x} \int_{-1}^1 \int_{-h}^0 p_o dz dy'. \quad (2.141)$$

We move terms around and simplify to obtain

$$bN_0 + \frac{1}{2} \frac{\partial}{\partial x} b \frac{\partial N_0}{\partial x} \int_{-1}^1 \int_{-h}^0 p_o dz dy' = 0. \quad (2.142)$$

Estuary width, b , is a function of along-channel position, x (Eq. (2.52)). So Eq. (2.142)

becomes

$$bN_0 + \frac{1}{2} \left(\frac{\partial b}{\partial x} \frac{\partial N_0}{\partial x} + b \frac{\partial^2 N_0}{\partial x^2} \right) \int_{-1}^1 \int_{-h}^0 p_o dz dy' = 0. \quad (2.143)$$

Let $P_o = \int_{-h}^0 p_o dz$, which is evaluated as

$$P_o = h + \frac{1}{\Gamma} \frac{\sinh(-\Gamma h)}{\cosh(\Gamma h) + \frac{\Gamma}{\delta} \sinh(\Gamma h)}. \quad (2.144)$$

Applying $\sinh(-z) = -\sinh(z)$, we have

$$P_o = h - \frac{1}{\Gamma} \frac{\sinh(\Gamma h)}{\cosh(\Gamma h) + \frac{\Gamma}{\delta} \sinh(\Gamma h)}. \quad (2.145)$$

So Eq. (2.143) becomes

$$bN_0 + \frac{1}{2} \left(\frac{\partial b}{\partial x} \frac{\partial N_0}{\partial x} + b \frac{\partial^2 N_0}{\partial x^2} \right) \int_{-1}^1 P_o dy' = 0. \quad (2.146)$$

We define κ_0^2 as

$$\kappa_0^2 = 2 \left(\int_{-1}^1 P_o dy' \right)^{-1}. \quad (2.147)$$

Then, we have

$$bN_0 + \frac{1}{\kappa_0^2} \left(\frac{\partial b}{\partial x} \frac{\partial N_0}{\partial x} + b \frac{\partial^2 N_0}{\partial x^2} \right) = 0. \quad (2.148)$$

Eq. (2.148) is rearranged:

$$\frac{b}{\kappa_0^2} \frac{\partial^2 N_0}{\partial x^2} + \frac{1}{\kappa_0^2} \frac{\partial b}{\partial x} \frac{\partial N_0}{\partial x} + bN_0 = 0. \quad (2.149)$$

Multiplying by $\frac{\kappa_0^2}{b}$, we have

$$\frac{\partial^2 N_0}{\partial x^2} + \frac{1}{b} \frac{\partial b}{\partial x} \frac{\partial N_0}{\partial x} + \kappa_0^2 N_0 = 0. \quad (2.150)$$

Substituting Eq. (2.52) and evaluating, we have an homogeneous ordinary differential equation,

$$\frac{d^2 N_0}{dx^2} - \mu \frac{dN_0}{dx} + \kappa_0^2 N_0 = 0. \quad (2.151)$$

We substitute $N_0 = e^{rx}$ to obtain the characteristic equation: $r^2 - \mu r + \kappa_0^2 = 0$.

From the quadratic equation, we find the complex roots to be

$$r = \frac{\mu}{2} \pm \sqrt{\kappa_0^2 - \frac{\mu^2}{4}}. \quad (2.152)$$

Let $d_0 = \kappa_0^2 - \frac{\mu^2}{4}$. Then, the solution for N_0 is

$$N_0 = C_1 e^{\frac{\mu x}{2}} (\cos(d_0 x) + i \sin(d_0 x)) + C_2 e^{\frac{\mu x}{2}} (\cos(d_0 x) - i \sin(d_0 x)). \quad (2.153)$$

To solve for the constants, C_1 and C_2 , we apply the boundary conditions, Eqs. (2.121) and (2.122). Applying Eq. (2.121), we have that $C_1 = 1 - C_2$, which we substitute into Eq. (2.153). After simplification, the solution becomes

$$N_0 = e^{\frac{\mu x}{2}} (\cos(d_0 x) + i \sin(d_0 x)) - 2i C_2 e^{\frac{\mu x}{2}} \sin(d_0 x). \quad (2.154)$$

After substituting the solution for U_0 integrated over depth, P_o , into Eq. (2.122), we have the condition (at $x = l$) that

$$\frac{dN_0}{dx} = 0. \quad (2.155)$$

To solve for C_2 , we take the derivative with respect to x of Eq. (2.154),

$$\begin{aligned} \frac{dN_0}{dx} = \frac{\mu}{2} e^{\frac{\mu x}{2}} (\cos(d_0 x) + i \sin(d_0 x)) + e^{\frac{\mu x}{2}} (-d_0 \sin(d_0 x) + i d_0 \cos(d_0 x)) - \\ 2i C_2 \left(\frac{\mu}{2} e^{\frac{\mu x}{2}} \sin(d_0 x) + d_0 e^{\frac{\mu x}{2}} \cos(d_0 x) \right). \end{aligned} \quad (2.156)$$

In the following four equations, we apply Eq. (2.155) and solve for C_2 :

$$\begin{aligned} 0 = \frac{\mu}{2} e^{\frac{\mu l}{2}} (\cos(d_0 l) + i \sin(d_0 l)) + e^{\frac{\mu l}{2}} (-d_0 \sin(d_0 l) + i d_0 \cos(d_0 l)) - \\ 2i C_2 \left(\frac{\mu}{2} e^{\frac{\mu l}{2}} \sin(d_0 l) + d_0 e^{\frac{\mu l}{2}} \cos(d_0 l) \right). \end{aligned} \quad (2.157)$$

$$\begin{aligned} 0 = \frac{\mu}{2} (\cos(d_0 l) + i \sin(d_0 l)) + (-d_0 \sin(d_0 l) + i d_0 \cos(d_0 l)) \\ - 2i C_2 \left(\frac{\mu}{2} \sin(d_0 l) + d_0 \cos(d_0 l) \right). \end{aligned} \quad (2.158)$$

$$2i C_2 \left(\frac{\mu}{2} \sin(d_0 l) + d_0 \cos(d_0 l) \right) = \left(\frac{\mu}{2} + i d_0 \right) \cos(d_0 l) - (d_0 - i \frac{\mu}{2}) \sin(d_0 l) \quad (2.159)$$

$$C_2 = \frac{\left(\frac{\mu}{2} + i d_0 \right) \cos(d_0 l) - (d_0 - i \frac{\mu}{2}) \sin(d_0 l)}{2i \left(\frac{\mu}{2} \sin(d_0 l) + d_0 \cos(d_0 l) \right)}. \quad (2.160)$$

Lastly, we substitute C_2 into Eq. (2.154).

$$\begin{aligned} N_0 = e^{\frac{\mu x}{2}} (\cos(d_0 x) + i \sin(d_0 x)) - \\ \frac{\left(\frac{\mu}{2} + i d_0 \right) \cos(d_0 l) - (d_0 - i \frac{\mu}{2}) \sin(d_0 l)}{\frac{\mu}{2} \sin(d_0 l) + d_0 \cos(d_0 l)} e^{\frac{\mu x}{2}} \sin(d_0 x). \end{aligned} \quad (2.161)$$

Eq. (2.161) is simplified in Eqs. (2.162) and (2.163)

$$\begin{aligned} N_0 = e^{\frac{\mu x}{2}} \left(\frac{(\cos(d_0 x) + i \sin(d_0 x)) \left(\frac{\mu}{2} \sin(d_0 l) + d_0 \cos(d_0 l) \right) - \\ \frac{\left(\frac{\mu}{2} + i d_0 \right) \cos(d_0 l) - (d_0 - i \frac{\mu}{2}) \sin(d_0 l) \sin(d_0 x)}{\frac{\mu}{2} \sin(d_0 l) + d_0 \cos(d_0 l)}}{\frac{\mu}{2} \sin(d_0 l) + d_0 \cos(d_0 l)} \right) \end{aligned} \quad (2.162)$$

$$N_0 = e^{\frac{\mu x}{2}} \left(\frac{\frac{\mu}{2}(\sin(d_0 l)\cos(d_0 x) - \cos(d_0 l)\sin(d_0 x))}{\frac{\mu}{2}\sin(d_0 l) + d_0\cos(d_0 l)} + \frac{d_0(\cos(d_0 l)\cos(d_0 x) + \sin(d_0 l)\sin(d_0 x))}{\frac{\mu}{2}\sin(d_0 l) + d_0\cos(d_0 l)} \right). \quad (2.163)$$

Applying the trigonometric identities $\sin(\alpha - \beta) = \sin(\alpha)\cos(\beta) - \cos(\alpha)\sin(\beta)$ and $\cos(\alpha - \beta) = \cos(\alpha)\cos(\beta) + \sin(\alpha)\sin(\beta)$, we have the final solution for N_0 , given by

$$N_0 = e^{\frac{\mu x}{2}} \left(\frac{\frac{\mu}{2}\sin(d_0(l-x)) + d_0\cos(d_0(l-x))}{\frac{\mu}{2}\sin(d_0 l) + d_0\cos(d_0 l)} \right). \quad (2.164)$$

Note that N_0 is a function of only x . We can now find $\frac{dN_0}{dx}$, which can then be substituted into the solution for U_0 , Eq. (2.137).

$$\begin{aligned} \frac{dN_0}{dx} &= \frac{\mu}{2} e^{\frac{\mu x}{2}} \left(\frac{\frac{\mu}{2}\sin(d_0(l-x)) + d_0\cos(d_0(l-x))}{\frac{\mu}{2}\sin(d_0 l) + d_0\cos(d_0 l)} \right) \\ &+ e^{\frac{\mu x}{2}} \left(\frac{d_0^2\sin(d_0(l-x)) - \frac{d_0\mu}{2}\cos(d_0(l-x))}{\frac{\mu}{2}\sin(d_0 l) + d_0\cos(d_0 l)} \right). \end{aligned} \quad (2.165)$$

2.1.4.3 Across-Channel Velocity

Next, we solve Eq. (2.109) for V_0 and apply boundary conditions Eqs. (2.115),(2.118).

We rearrange terms and multiply by $\frac{2}{\alpha A_v}$

$$\frac{\partial^2 v_0}{\partial z^2} + \frac{2i}{A_v} V_0 = \frac{2f}{\alpha A_v} U_0 + \frac{2\epsilon}{\alpha^2 A_v} \frac{\partial N'}{\partial y} - \frac{2\epsilon}{\alpha A_v} \int_{-h}^0 \frac{\partial \hat{\rho}_1}{\partial y} dz. \quad (2.166)$$

Recall, $\Gamma^2 = \frac{-2i}{A_v}$. We replace the lateral density gradient by the lateral gradient of the depth-mean density.

$$\frac{\partial^2 V_0}{\partial z^2} - \Gamma^2 V_0 = \frac{2f}{\alpha A_v} U_0 + \frac{2\epsilon}{\alpha^2 A_v} \frac{\partial N'}{\partial y} - \frac{2\epsilon}{\alpha A_v} \frac{\partial}{\partial y} \left(\frac{1}{h} \int_{-h}^0 \hat{\rho}_1 dz \right) z. \quad (2.167)$$

The solution for V_0 is a linear combination of the solutions to the homogeneous and non-homogeneous equations, i.e. $V_0 = V_{0,h} + V_{0,nh}$. The solution to the homogeneous equation, $V_{0,h}$, found from the characteristic equation, is given by

$$V_{0,h} = C_1 e^{\Gamma z} + C_2 e^{-\Gamma z}. \quad (2.168)$$

The solution to the non-homogeneous equation is a combination of three parts, each corresponding to a term on the right hand side of Eq. (2.167), i.e.

$V_{0,nh} = V_{0,nh_1} + V_{0,nh_2} + V_{0,nh_3}$. We use undetermined coefficients to find V_{0,nh_2} and V_{0,nh_3} . Note that A, B, C are constants.

$$V_{0,nh_2} = A \frac{\partial N'}{\partial y},$$

implying that

$$0 - \Gamma^2 A \frac{\partial N'}{\partial y} = \frac{2\epsilon}{\alpha^2 A_v} \frac{\partial N'}{\partial y}$$

from which it follows that

$$V_{0,nh_2} = -\frac{i\epsilon}{\alpha^2} \frac{\partial N'}{\partial y}. \quad (2.169)$$

$$V_{0,nh_3} = B \frac{\partial}{\partial y} \left(\frac{1}{h} \int_{-h}^0 \hat{\rho}_1 dz \right) z + C,$$

implying that

$$0 - \Gamma^2 \left(B \frac{\partial}{\partial y} \left(\frac{1}{h} \int_{-h}^0 \hat{\rho}_1 dz \right) z + C \right) = -\frac{2\epsilon}{\alpha A_v} \frac{\partial}{\partial y} \left(\frac{1}{h} \int_{-h}^0 \hat{\rho}_1 dz \right) z$$

from which it follows

$$V_{0,nh_3} = \frac{i\epsilon}{\alpha} \frac{\partial}{\partial y} \left(\frac{1}{h} \int_{-h}^0 \hat{\rho}_1 dz \right) z. \quad (2.170)$$

V_{0,nh_1} is found from the solution to the homogeneous equation, Eq. (2.168), using variation of parameters. The solution for V_{0,nh_1} can be written as

$$V_{0,nh_1} = u_1 e^{\Gamma z} + u_2 e^{-\Gamma z}, \quad (2.171)$$

where $u_1, u_2 = f(x, y, z)$. Note that u_1, u_2 are not the first order and second order expansions of the along-channel velocity. The system of equations we will use to solve for u_1, u_2 is given by

$$\begin{aligned} u_1' e^{\Gamma z} + u_2' e^{-\Gamma z} &= 0 \\ \Gamma u_1' e^{\Gamma z} - \Gamma u_2' e^{-\Gamma z} &= g(x, y, z), \end{aligned} \quad (2.172)$$

where $g(x, y, z) = \frac{-2if}{\alpha A_v} \frac{dN_0}{dx} \left(1 - \frac{\cosh(\Gamma z)}{\cosh(\Gamma h) + \frac{\Gamma}{\delta} \sinh(\Gamma h)} \right)$. Then,

$$\begin{aligned} u_1 &= - \int \frac{e^{-\Gamma z} g(x, y, z)}{W} dz \\ u_2 &= \int \frac{e^{\Gamma z} g(x, y, z)}{W} dz, \end{aligned} \quad (2.173)$$

where W is the Wronskian of $e^{\Gamma z}$ and $e^{-\Gamma z}$ given by

$$W = -2\Gamma. \quad (2.174)$$

We integrate over depth to solve for u_1 and u_2 , noting that h is constant with depth.

$$u_1 = - \frac{if}{\Gamma \alpha A_v} \frac{dN_0}{dx} \int \left(e^{-\Gamma z} - \frac{e^{-\Gamma z} \cosh(\Gamma z)}{\cosh(\Gamma h) + \frac{\Gamma}{\delta} \sinh(\Gamma h)} \right) dz, \quad (2.175)$$

$$u_1 = - \frac{if}{\Gamma \alpha A_v} \frac{dN_0}{dx} \left(\frac{-1}{\Gamma} e^{-\Gamma z} - \int \frac{e^{-\Gamma z} (e^{\Gamma z} + e^{-\Gamma z})}{2(\cosh(\Gamma h) + \frac{\Gamma}{\delta} \sinh(\Gamma h))} dz \right), \quad (2.176)$$

$$u_1 = - \frac{if}{\Gamma \alpha A_v} \frac{dN_0}{dx} \left(\frac{-1}{\Gamma} e^{-\Gamma z} - \int \frac{1 + e^{-2\Gamma z}}{2(\cosh(\Gamma h) + \frac{\Gamma}{\delta} \sinh(\Gamma h))} dz \right), \quad (2.177)$$

$$\begin{aligned} u_1 &= \frac{if}{\Gamma^2 \alpha A_v} \frac{dN_0}{dx} e^{-\Gamma z} + \frac{if}{2\Gamma \alpha A_v (\cosh(\Gamma h) + \frac{\Gamma}{\delta} \sinh(\Gamma h))} \frac{dN_0}{dx} z \\ &\quad - \frac{if}{4\Gamma^2 \alpha A_v} \frac{dN_0}{dx} \frac{e^{-2\Gamma z}}{\cosh(\Gamma h) + \frac{\Gamma}{\delta} \sinh(\Gamma h)}. \end{aligned} \quad (2.178)$$

Recall, $\Gamma^2 = -\frac{2i}{A_v}$. Then, the final solution for u_1 is

$$\begin{aligned} u_1 &= \frac{-f}{2\alpha} \frac{dN_0}{dx} e^{-\Gamma z} - \frac{f}{4\alpha} \frac{dN_0}{dx} \frac{\Gamma z}{\cosh(\Gamma h) + \frac{\Gamma}{\delta} \sinh(\Gamma h)} \\ &\quad + \frac{f}{8\alpha} \frac{dN_0}{dx} \frac{e^{-2\Gamma z}}{\cosh(\Gamma h) + \frac{\Gamma}{\delta} \sinh(\Gamma h)}. \end{aligned} \quad (2.179)$$

It follows similarly that the solution for u_2 is given by

$$\begin{aligned} u_2 &= \frac{-f}{2\alpha} \frac{dN_0}{dx} e^{\Gamma z} + \frac{f}{4\alpha} \frac{dN_0}{dx} \frac{\Gamma z}{\cosh(\Gamma h) + \frac{\Gamma}{\delta} \sinh(\Gamma h)} \\ &\quad + \frac{f}{8\alpha} \frac{dN_0}{dx} \frac{e^{2\Gamma z}}{\cosh(\Gamma h) + \frac{\Gamma}{\delta} \sinh(\Gamma h)}. \end{aligned} \quad (2.180)$$

Substituting these into Eq. (2.171) and simplifying, we have

$$V_{0,nh_1} = \frac{f}{\alpha} \left(\frac{1}{4} \frac{\cosh(\Gamma z)}{\cosh(\Gamma h) + \frac{\Gamma}{\delta} \sinh(\Gamma h)} - \frac{1}{2} \frac{\Gamma z \sinh(\Gamma z)}{\cosh(\Gamma h) + \frac{\Gamma}{\delta} \sinh(\Gamma h)} - 1 \right) \frac{dN_0}{dx}. \quad (2.181)$$

Combining the solutions to the homogeneous and non-homogeneous solution, the solution for V_0 is given by

$$V_0 = C_1 e^{\Gamma z} + C_2 e^{-\Gamma z} + \frac{f}{\alpha} \left(\frac{1}{4} \frac{\cosh(\Gamma z)}{\cosh(\Gamma h) + \frac{\Gamma}{\delta} \sinh(\Gamma h)} - \frac{1}{2} \frac{\Gamma z \sinh(\Gamma z)}{\cosh(\Gamma h) + \frac{\Gamma}{\delta} \sinh(\Gamma h)} - 1 \right) \frac{dN_0}{dx} - \frac{i\epsilon}{\alpha^2} \frac{\partial N'}{\partial y} + \frac{i\epsilon}{\alpha} \frac{\partial}{\partial y} \left(\frac{1}{h} \int_{-h}^0 \hat{\rho}_1 dz \right) z, \quad (2.182)$$

with its first partial derivative with respect to z given by

$$\begin{aligned} \frac{\partial V_0}{\partial z} &= \Gamma C_1 e^{\Gamma z} - \Gamma C_2 e^{-\Gamma z} \\ &+ \frac{f}{\alpha} \left(\frac{\Gamma}{4} \frac{\sinh(\Gamma z)}{\cosh(\Gamma h) + \frac{\Gamma}{\delta} \sinh(\Gamma h)} - \frac{\Gamma \sinh(\Gamma z) + \Gamma z \cosh(\Gamma z)}{2 \cosh(\Gamma h) + \frac{\Gamma}{\delta} \sinh(\Gamma h)} \right) \frac{dN_0}{dx} \\ &+ \frac{i\epsilon}{\alpha} \frac{\partial}{\partial y} \left(\frac{1}{h} \int_{-h}^0 \hat{\rho}_1 dz \right). \end{aligned} \quad (2.183)$$

To solve for C_1, C_2 , first, we apply the surface boundary condition, Eq. (2.115),

$$0 = \Gamma C_1 - \Gamma C_2 + \frac{i\epsilon}{\alpha} \frac{\partial}{\partial y} \left(\frac{1}{h} \int_{-h}^0 \hat{\rho}_1 dz \right). \quad (2.184)$$

C_2 is, thus, given by

$$C_2 = C_1 + \frac{i\epsilon}{\Gamma \alpha} \frac{\partial}{\partial y} \left(\frac{1}{h} \int_{-h}^0 \hat{\rho}_1 dz \right). \quad (2.185)$$

So V_0 and $\frac{\partial V_0}{\partial z}$ can be written as

$$\begin{aligned} V_0 &= 2C_1 \cosh(\Gamma z) + \frac{i\epsilon}{\Gamma \alpha} e^{-\Gamma z} \frac{\partial}{\partial y} \left(\frac{1}{h} \int_{-h}^0 \hat{\rho}_1 dz \right) \\ &+ \frac{f}{\alpha} \left(\frac{1}{4} \frac{\cosh(\Gamma z)}{\cosh(\Gamma h) + \frac{\Gamma}{\delta} \sinh(\Gamma h)} - \frac{1}{2} \frac{\Gamma z \sinh(\Gamma z)}{\cosh(\Gamma h) + \frac{\Gamma}{\delta} \sinh(\Gamma h)} - 1 \right) \frac{dN_0}{dx} \\ &- \frac{i\epsilon}{\alpha^2} \frac{\partial N'}{\partial y} + \frac{i\epsilon}{\alpha} \frac{\partial}{\partial y} \left(\frac{1}{h} \int_{-h}^0 \hat{\rho}_1 dz \right) z \end{aligned} \quad (2.186)$$

$$\begin{aligned}
\frac{\partial V_0}{\partial z} &= 2\Gamma C_1 \sinh(\Gamma z) - \frac{i\epsilon}{\alpha} e^{-\Gamma z} \frac{\partial}{\partial y} \left(\frac{1}{h} \int_{-h}^0 \hat{\rho}_1 dz \right) \\
+ \frac{f}{\alpha} &\left(\frac{\Gamma}{4} \frac{\sinh(\Gamma z)}{\cosh(\Gamma h) + \frac{\Gamma}{\delta} \sinh(\Gamma h)} - \frac{\Gamma \sinh(\Gamma z) + \Gamma z \cosh(\Gamma z)}{2 \cosh(\Gamma h) + \frac{\Gamma}{\delta} \sinh(\Gamma h)} \right) \frac{dN_0}{dx} \\
&+ \frac{i\epsilon}{\alpha} \frac{\partial}{\partial y} \left(\frac{1}{h} \int_{-h}^0 \hat{\rho}_1 dz \right).
\end{aligned} \tag{2.187}$$

Now, we apply the bottom boundary condition, Eq. (2.118), to solve for C_1 :

$$\begin{aligned}
2C_1 \cosh(-\Gamma h) &+ \frac{i\epsilon}{\Gamma\alpha} e^{\Gamma h} \frac{\partial}{\partial y} \left(\frac{1}{h} \int_{-h}^0 \hat{\rho}_1 dz \right) \\
+ \frac{f}{\alpha} &\left(\frac{1}{4} \frac{\cosh(-\Gamma h)}{\cosh(\Gamma h) + \frac{\Gamma}{\delta} \sinh(\Gamma h)} - \frac{1}{2} \frac{-\Gamma h \sinh(-\Gamma h)}{\cosh(\Gamma h) + \frac{\Gamma}{\delta} \sinh(\Gamma h)} - 1 \right) \frac{dN_0}{dx} \\
&- \frac{i\epsilon}{\alpha^2} \frac{\partial N'}{\partial y} - \frac{i\epsilon h}{\alpha} \frac{\partial}{\partial y} \left(\frac{1}{h} \int_{-h}^0 \hat{\rho}_1 dz \right) = \\
2\frac{\Gamma}{\delta} C_1 \sinh(-\Gamma h) &- \frac{i\epsilon}{\delta\alpha} e^{\Gamma h} \frac{\partial}{\partial y} \left(\frac{1}{h} \int_{-h}^0 \hat{\rho}_1 dz \right) \\
+ \frac{f}{\alpha} &\left(\frac{\Gamma}{4\delta} \frac{\sinh(-\Gamma h)}{\cosh(\Gamma h) + \frac{\Gamma}{\delta} \sinh(\Gamma h)} - \frac{\Gamma \sinh(-\Gamma h) - \Gamma h \cosh(-\Gamma h)}{2\delta \cosh(\Gamma h) + \frac{\Gamma}{\delta} \sinh(\Gamma h)} \right) \frac{dN_0}{dx} \\
&+ \frac{i\epsilon}{\delta\alpha} \frac{\partial}{\partial y} \left(\frac{1}{h} \int_{-h}^0 \hat{\rho}_1 dz \right).
\end{aligned} \tag{2.188}$$

$$\begin{aligned}
& 2C_1 \cosh(\Gamma h) + \frac{i\epsilon}{\Gamma\alpha} e^{\Gamma h} \frac{\partial}{\partial y} \left(\frac{1}{h} \int_{-h}^0 \hat{\rho}_1 dz \right) \\
+ \frac{f}{\alpha} & \left(\frac{1}{4} \frac{\cosh(\Gamma h)}{\cosh(\Gamma h) + \frac{\Gamma}{\delta} \sinh(\Gamma h)} - \frac{1}{2} \frac{\Gamma h \sinh(\Gamma h)}{\cosh(\Gamma h) + \frac{\Gamma}{\delta} \sinh(\Gamma h)} - 1 \right) \frac{dN_0}{dx} \\
& - \frac{i\epsilon}{\alpha^2} \frac{\partial N'}{\partial y} - \frac{i\epsilon h}{\alpha} \frac{\partial}{\partial y} \left(\frac{1}{h} \int_{-h}^0 \hat{\rho}_1 dz \right) = \\
& - 2 \frac{\Gamma}{\delta} C_1 \sinh(\Gamma h) - \frac{i\epsilon}{\delta\alpha} e^{\Gamma h} \frac{\partial}{\partial y} \left(\frac{1}{h} \int_{-h}^0 \hat{\rho}_1 dz \right) \\
+ \frac{f}{\alpha} & \left(\frac{-\Gamma}{4\delta} \frac{\sinh(\Gamma h)}{\cosh(\Gamma h) + \frac{\Gamma}{\delta} \sinh(\Gamma h)} + \frac{\Gamma \sinh(\Gamma h) + \Gamma h \cosh(\Gamma h)}{2\delta \cosh(\Gamma h) + \frac{\Gamma}{\delta} \sinh(\Gamma h)} \right) \frac{dN_0}{dx} \\
& + \frac{i\epsilon}{\delta\alpha} \frac{\partial}{\partial y} \left(\frac{1}{h} \int_{-h}^0 \hat{\rho}_1 dz \right).
\end{aligned} \tag{2.189}$$

$$\begin{aligned}
2C_1 & \left(\cosh(\Gamma h) + \frac{\Gamma}{\delta} \sinh(\Gamma h) \right) = - \frac{i\epsilon}{\Gamma\alpha} e^{\Gamma h} \frac{\partial}{\partial y} \left(\frac{1}{h} \int_{-h}^0 \hat{\rho}_1 dz \right) \\
& + \frac{i\epsilon h}{\alpha} \frac{\partial}{\partial y} \left(\frac{1}{h} \int_{-h}^0 \hat{\rho}_1 dz \right) + \frac{i\epsilon}{\alpha^2} \frac{\partial N'}{\partial y} - \frac{f}{\alpha} \left(\frac{1}{4} \frac{\cosh(\Gamma h)}{\cosh(\Gamma h) + \frac{\Gamma}{\delta} \sinh(\Gamma h)} \right. \\
& - \left. \frac{1}{2} \frac{\Gamma h \sinh(\Gamma h)}{\cosh(\Gamma h) + \frac{\Gamma}{\delta} \sinh(\Gamma h)} - 1 \right) \frac{dN_0}{dx} - \frac{i\epsilon}{\delta\alpha} e^{\Gamma h} \frac{\partial}{\partial y} \left(\frac{1}{h} \int_{-h}^0 \hat{\rho}_1 dz \right) \\
& + \frac{i\epsilon}{\delta\alpha} \frac{\partial}{\partial y} \left(\frac{1}{h} \int_{-h}^0 \hat{\rho}_1 dz \right) + \frac{f}{\alpha} \left(\frac{-\Gamma}{4\delta} \frac{\sinh(\Gamma h)}{\cosh(\Gamma h) + \frac{\Gamma}{\delta} \sinh(\Gamma h)} \right. \\
& + \left. \frac{\Gamma \sinh(\Gamma h) + \Gamma h \cosh(\Gamma h)}{2\delta \cosh(\Gamma h) + \frac{\Gamma}{\delta} \sinh(\Gamma h)} \right) \frac{dN_0}{dx}.
\end{aligned} \tag{2.190}$$

$$\begin{aligned}
2C_1 & \left(\cosh(\Gamma h) + \frac{\Gamma}{\delta} \sinh(\Gamma h) \right) = \frac{i\epsilon}{\alpha} \left(- \frac{e^{\Gamma h}}{\Gamma} - \frac{e^{\Gamma h}}{\delta} + h + \frac{1}{\delta} \right) \\
& \frac{\partial}{\partial y} \left(\frac{1}{h} \int_{-h}^0 \hat{\rho}_1 dz \right) + \frac{i\epsilon}{\alpha^2} \frac{\partial N'}{\partial y} \\
+ \frac{f}{\alpha} & \left(- \frac{1}{4} \frac{\cosh(\Gamma h)}{\cosh(\Gamma h) + \frac{\Gamma}{\delta} \sinh(\Gamma h)} + \frac{\Gamma h}{2} \frac{\sinh(\Gamma h)}{\cosh(\Gamma h) + \frac{\Gamma}{\delta} \sinh(\Gamma h)} + 1 \right) \frac{dN_0}{dx} \\
& + \frac{f}{\alpha} \left(\frac{-\Gamma}{4\delta} \frac{\sinh(\Gamma h)}{\cosh(\Gamma h) + \frac{\Gamma}{\delta} \sinh(\Gamma h)} + \frac{\Gamma \sinh(\Gamma h) + \Gamma h \cosh(\Gamma h)}{2\delta \cosh(\Gamma h) + \frac{\Gamma}{\delta} \sinh(\Gamma h)} \right) \frac{dN_0}{dx}.
\end{aligned} \tag{2.191}$$

$$\begin{aligned}
2C_1(\cosh(\Gamma h) + \frac{\Gamma}{\delta}\sinh(\Gamma h)) &= \frac{i\epsilon}{\alpha} \left(-\frac{e^{\Gamma h}}{\Gamma} - \frac{e^{\Gamma h}}{\delta} + h + \frac{1}{\delta} \right) \\
\frac{\partial}{\partial y} \left(\frac{1}{h} \int_{-h}^0 \hat{\rho}_1 dz \right) + \frac{i\epsilon}{\alpha^2} \frac{\partial N'}{\partial y} + \frac{f}{\alpha} \left(1 + \frac{1}{\cosh(\Gamma h) + \frac{\Gamma}{\delta}\sinh(\Gamma h)} \right. \\
&\left. \left(\sinh(\Gamma h) \left(-\frac{\Gamma}{4\delta} + \frac{\Gamma}{2\delta} + \frac{\Gamma h}{2} \right) + \cosh(\Gamma h) \left(\frac{\Gamma^2 h}{2\delta} - \frac{1}{4} \right) \right) \right) \frac{dN_0}{dx}
\end{aligned} \tag{2.192}$$

The solution for C_1 is given by

$$\begin{aligned}
C_1 &= \frac{1}{2(\cosh(\Gamma h) + \frac{\Gamma}{\delta}\sinh(\Gamma h))} \frac{i\epsilon}{\alpha} \left(-\frac{e^{\Gamma h}}{\Gamma} - \frac{e^{\Gamma h}}{\delta} + h + \frac{1}{\delta} \right) \\
&\frac{\partial}{\partial y} \left(\frac{1}{h} \int_{-h}^0 \hat{\rho}_1 dz \right) + \frac{1}{2(\cosh(\Gamma h) + \frac{\Gamma}{\delta}\sinh(\Gamma h))} \frac{i\epsilon}{\alpha^2} \frac{\partial N'}{\partial y} \\
&+ \frac{1}{2(\cosh(\Gamma h) + \frac{\Gamma}{\delta}\sinh(\Gamma h))} \frac{f}{\alpha} \left[1 + \frac{1}{\cosh(\Gamma h) + \frac{\Gamma}{\delta}\sinh(\Gamma h)} \right. \\
&\left. \left(\sinh(\Gamma h) \left(-\frac{\Gamma}{4\delta} + \frac{\Gamma}{2\delta} + \frac{\Gamma h}{2} \right) + \cosh(\Gamma h) \left(\frac{\Gamma^2 h}{2\delta} - \frac{1}{4} \right) \right) \right] \frac{dN_0}{dx}.
\end{aligned} \tag{2.193}$$

We substitute C_1 into Eq. (2.186) and group terms:

$$\begin{aligned}
V_0 &= \frac{f}{\alpha} \left[\frac{\cosh(\Gamma z)}{\cosh(\Gamma h) + \frac{\Gamma}{\delta}\sinh(\Gamma h)} \left[1 + \frac{1}{\cosh(\Gamma h) + \frac{\Gamma}{\delta}\sinh(\Gamma h)} \right. \right. \\
&\left. \left. \left(\sinh(\Gamma h) \left(-\frac{\Gamma}{4\delta} + \frac{\Gamma}{2\delta} + \frac{\Gamma h}{2} \right) + \cosh(\Gamma h) \left(\frac{\Gamma^2 h}{2\delta} - \frac{1}{4} \right) \right) \right] \right. \\
&+ \left. \frac{1}{\cosh(\Gamma h) + \frac{\Gamma}{\delta}\sinh(\Gamma h)} \left(\frac{1}{4}\cosh(\Gamma z) - \frac{\Gamma z}{2}\sinh(\Gamma z) \right) - 1 \right] \frac{dN_0}{dx} \\
&+ \frac{i\epsilon}{\alpha} \left[\frac{\cosh(\Gamma z)}{\cosh(\Gamma h) + \frac{\Gamma}{\delta}\sinh(\Gamma h)} \left(-\frac{e^{\Gamma h}}{\Gamma} - \frac{e^{\Gamma h}}{\delta} + h + \frac{1}{\delta} \right) + \frac{e^{-\Gamma z}}{\Gamma} + z \right] \\
&\frac{\partial}{\partial y} \left(\frac{1}{h} \int_{-h}^0 \hat{\rho}_1 dz \right) + \frac{i\epsilon}{\alpha^2} \left[\frac{\cosh(\Gamma z)}{\cosh(\Gamma h) + \frac{\Gamma}{\delta}\sinh(\Gamma h)} - 1 \right] \frac{\partial N'}{\partial y}.
\end{aligned} \tag{2.194}$$

In the next several equations, we simplify the solution

$$\begin{aligned}
V_0 = & \frac{f}{\alpha} \left[\frac{\cosh(\Gamma z)}{\cosh(\Gamma h) + \frac{\Gamma}{\delta} \sinh(\Gamma h)} \left[1 + \frac{1}{\cosh(\Gamma h) + \frac{\Gamma}{\delta} \sinh(\Gamma h)} \right. \right. \\
& \left. \left(\sinh(\Gamma h) \left(-\frac{\Gamma}{4\delta} + \frac{\Gamma}{2\delta} + \frac{\Gamma h}{2} \right) + \cosh(\Gamma h) \left(\frac{\Gamma^2 h}{2\delta} - \frac{1}{4} \right) \right) \right] \\
& + \frac{1}{\cosh(\Gamma h) + \frac{\Gamma}{\delta} \sinh(\Gamma h)} \left(\frac{1}{4} \cosh(\Gamma z) - \frac{\Gamma z}{2} \sinh(\Gamma z) \right) - 1 \Big] \frac{dN_0}{dx} \\
& + \frac{i\epsilon}{\alpha} \left[\frac{\cosh(\Gamma z)}{\cosh(\Gamma h) + \frac{\Gamma}{\delta} \sinh(\Gamma h)} \left(-\frac{\cosh(\Gamma h) + \sinh(\Gamma h)}{\Gamma} \right. \right. \\
& \left. \left. - \frac{\cosh(\Gamma h) + \sinh(\Gamma h)}{\delta} + h + \frac{1}{\delta} \right) + \frac{1}{\Gamma} \left(\cosh(\Gamma z) - \sinh(\Gamma z) \right) + z \right] \\
& \frac{\partial}{\partial y} \left(\frac{1}{h} \int_{-h}^0 \hat{\rho}_1 dz \right) + \frac{i\epsilon}{\alpha^2} \left[\frac{\cosh(\Gamma z)}{\cosh(\Gamma h) + \frac{\Gamma}{\delta} \sinh(\Gamma h)} - 1 \right] \frac{\partial N'}{\partial y}
\end{aligned} \tag{2.195}$$

$$\begin{aligned}
V_0 = & \frac{f}{\alpha} \frac{\cosh(\Gamma z)}{\cosh(\Gamma h) + \frac{\Gamma}{\delta} \sinh(\Gamma h)} \left[1 + \frac{1}{\cosh(\Gamma h) + \frac{\Gamma}{\delta} \sinh(\Gamma h)} \right. \\
& \left. \left(\sinh(\Gamma h) \left(-\frac{\Gamma}{4\delta} + \frac{\Gamma}{2\delta} + \frac{\Gamma h}{2} \right) + \cosh(\Gamma h) \left(\frac{\Gamma^2 h}{2\delta} - \frac{1}{4} \right) \right) \right] \\
& + \frac{1}{\cosh(\Gamma h) + \frac{\Gamma}{\delta} \sinh(\Gamma h)} \left(\frac{1}{4} \cosh(\Gamma z) - \frac{\Gamma z}{2} \sinh(\Gamma z) \right) - 1 \Big] \frac{dN_0}{dx} \\
& + \frac{i\epsilon}{\alpha} \left[\frac{\cosh(\Gamma z)}{\cosh(\Gamma h) + \frac{\Gamma}{\delta} \sinh(\Gamma h)} \left(-\frac{1}{\Gamma} \sinh(\Gamma h) - \frac{1}{\delta} \cosh(\Gamma h) + h + \frac{1}{\delta} \right) \right. \\
& \left. - \frac{1}{\Gamma} \sinh(\Gamma z) + z \right] \frac{\partial}{\partial y} \left(\frac{1}{h} \int_{-h}^0 \hat{\rho}_1 dz \right) \\
& + \frac{i\epsilon}{\alpha^2} \left[\frac{\cosh(\Gamma z)}{\cosh(\Gamma h) + \frac{\Gamma}{\delta} \sinh(\Gamma h)} - 1 \right] \frac{\partial N'}{\partial y}
\end{aligned} \tag{2.196}$$

$$\begin{aligned}
V_0 = & \frac{f}{\alpha(\cosh(\Gamma h) + \frac{\Gamma}{\delta}\sinh(\Gamma h))} \left[\frac{\cosh(\Gamma z)}{\cosh(\Gamma h) + \frac{\Gamma}{\delta}\sinh(\Gamma h)} \left(\cosh(\Gamma h) \right. \right. \\
& + \frac{\Gamma}{\delta}\sinh(\Gamma h) + \sinh(\Gamma h) \left(\frac{\Gamma}{4\delta} + \frac{\Gamma h}{2} \right) + \cosh(\Gamma h) \left(\frac{\Gamma^2 h}{2\delta} - \frac{1}{4} \right) \Big) \\
& + \frac{1}{4}\cosh(\Gamma z) - \frac{\Gamma z}{2}\sinh(\Gamma z) - \cosh(\Gamma h) - \frac{\Gamma}{\delta}\sinh(\Gamma h) \Big] \frac{dN_0}{dx} \\
& + \frac{i\epsilon}{\alpha} \left[\frac{\cosh(\Gamma z)}{\cosh(\Gamma h) + \frac{\Gamma}{\delta}\sinh(\Gamma h)} \left(-\frac{1}{\Gamma}\sinh(\Gamma h) - \frac{1}{\delta}\cosh(\Gamma h) + h + \frac{1}{\delta} \right) \right. \\
& \left. - \frac{1}{\Gamma}\sinh(\Gamma z) + z \right] \frac{\partial}{\partial y} \left(\frac{1}{h} \int_{-h}^0 \hat{\rho}_1 dz \right) \\
& + \frac{i\epsilon}{\alpha^2} \left[\frac{\cosh(\Gamma z)}{\cosh(\Gamma h) + \frac{\Gamma}{\delta}\sinh(\Gamma h)} - 1 \right] \frac{\partial N'}{\partial y}
\end{aligned} \tag{2.197}$$

$$\begin{aligned}
V_0 = & \frac{f}{\alpha(\cosh(\Gamma h) + \frac{\Gamma}{\delta}\sinh(\Gamma h))} \left[\frac{\cosh(\Gamma z)}{\cosh(\Gamma h) + \frac{\Gamma}{\delta}\sinh(\Gamma h)} \left(\cosh(\Gamma h) \right. \right. \\
& + \frac{\Gamma}{\delta}\sinh(\Gamma h) + \sinh(\Gamma h) \left(\frac{\Gamma}{4\delta} + \frac{\Gamma h}{2} \right) + \cosh(\Gamma h) \left(\frac{\Gamma^2 h}{2\delta} - \frac{1}{4} \right) \\
& \left. - \frac{3\Gamma}{4\delta}\sinh(\Gamma h) - \frac{3}{4}\cosh(\Gamma h) \right) + \frac{3\cosh(\Gamma z)}{4(\cosh(\Gamma h) + \frac{\Gamma}{\delta}\sinh(\Gamma h))} \\
& \left(\cosh(\Gamma h) + \frac{\Gamma}{\delta}\sinh(\Gamma h) \right) + \frac{1}{4}\cosh(\Gamma z) - \frac{\Gamma z}{2}\sinh(\Gamma z) \\
& \left. - \cosh(\Gamma h) - \frac{\Gamma}{\delta}\sinh(\Gamma h) \right] \frac{dN_0}{dx} + \frac{i\epsilon}{\alpha} \left[\frac{\cosh(\Gamma z)}{\cosh(\Gamma h) + \frac{\Gamma}{\delta}\sinh(\Gamma h)} \right. \\
& \left. \left(-\frac{1}{\Gamma}\sinh(\Gamma h) - \frac{1}{\delta}\cosh(\Gamma h) + h + \frac{1}{\delta} \right) \frac{1}{\Gamma}\sinh(\Gamma z) + z \right] \frac{\partial}{\partial y} \left(\frac{1}{h} \int_{-h}^0 \hat{\rho}_1 dz \right) \\
& + \frac{i\epsilon}{\alpha^2} \left[\frac{\cosh(\Gamma z)}{\cosh(\Gamma h) + \frac{\Gamma}{\delta}\sinh(\Gamma h)} - 1 \right] \frac{\partial N'}{\partial y}.
\end{aligned} \tag{2.198}$$

The final solution for V_0 is given by

$$\begin{aligned}
V_0 = & \frac{f}{\alpha(\cosh(\Gamma h) + \frac{\Gamma}{\delta}\sinh(\Gamma h))} \left[\frac{\cosh(\Gamma z)}{\cosh(\Gamma h) + \frac{\Gamma}{\delta}\sinh(\Gamma h)} \left(\cosh(\Gamma h) \right. \right. \\
& + \left. \frac{\Gamma}{\delta}\sinh(\Gamma h) + \sinh(\Gamma h) \left(\frac{\Gamma h}{2} - \frac{\Gamma}{2\delta} \right) + \cosh(\Gamma h) \left(\frac{\Gamma^2 h}{2\delta} - 1 \right) \right) \\
& + \left. \cosh(\Gamma z) - \frac{\Gamma z}{2}\sinh(\Gamma z) \cosh(\Gamma h) - \frac{\Gamma}{\delta}\sinh(\Gamma h) \right] \frac{dN_0}{dx} \\
& + \frac{i\epsilon}{\alpha} \left[\frac{\cosh(\Gamma z)}{\cosh(\Gamma h) + \frac{\Gamma}{\delta}\sinh(\Gamma h)} \left(-\frac{1}{\Gamma}\sinh(\Gamma h) - \frac{1}{\delta}\cosh(\Gamma h) + h + \frac{1}{\delta} \right) \right. \\
& - \left. \frac{1}{\Gamma}\sinh(\Gamma z) + z \right] \frac{\partial}{\partial y} \left(\frac{1}{h} \int_{-h}^0 \hat{\rho}_1 dz \right) \\
& + \frac{i\epsilon}{\alpha^2} \left[\frac{\cosh(\Gamma z)}{\cosh(\Gamma h) + \frac{\Gamma}{\delta}\sinh(\Gamma h)} - 1 \right] \frac{\partial N'}{\partial y}. \tag{2.199}
\end{aligned}$$

In consideration of the length, we will use the following identities in addition to p_0 , Eq. (2.140), to write V_0

$$F = \cosh(\Gamma h) + \frac{\Gamma}{\delta}\sinh(\Gamma h) \tag{2.200}$$

$$p_h = F + \sinh(\Gamma h) \left(\frac{\Gamma h}{2} - \frac{\Gamma}{2\delta} \right) + \cosh(\Gamma h) \left(\frac{\Gamma^2}{2\delta} - 1 \right) \tag{2.201}$$

$$p_z = \cosh(\Gamma z) - \frac{\Gamma z}{2}\sinh(\Gamma z) - F \tag{2.202}$$

$$r_h = -\frac{1}{\Gamma}\sinh(\Gamma h) - \frac{1}{\delta}\cosh(\Gamma h) + h + \frac{1}{\delta} \tag{2.203}$$

$$r_z = -\frac{1}{\Gamma}\sinh(\Gamma z) + z \tag{2.204}$$

So V_0 becomes

$$V_0 = \frac{f}{\alpha F} \left[(1-p_0)p_h + p_z \right] \frac{dN_0}{dx} + \frac{i\epsilon}{\alpha} \left[(1-p_0)r_h + r_z \right] \frac{\partial}{\partial y} \left(\frac{1}{h} \int_{-h}^0 \hat{\rho}_1 dz \right) - \frac{i\epsilon}{\alpha^2} p_0 \frac{\partial N'}{\partial y}. \tag{2.205}$$

It should be noted that p_h and p_z differ slightly from that of Ensing et al. (2015), which is the basis for this model's derivation. There is a F , where they have a 1 [4].

In order to solve for V_0 , we need to find $\frac{\partial N'}{\partial y}$. We integrate the continuity equation over depth and width (from $-\frac{b}{2}$ to $y'\frac{b}{2}$). We first integrate over depth and apply the surface and

bottom boundary conditions for vertical velocity, W_0 .

$$\int_{-h}^0 \left(\frac{\partial U_0}{\partial x} + \frac{\partial V_0}{\partial y} + \frac{\partial W_0}{\partial z} = 0 \right) dz \quad (2.206)$$

$$\int_{-h}^0 \frac{\partial U_0}{\partial x} dz + \int_{-h}^0 \frac{\partial V_0}{\partial y} dz + \int_{-h}^0 \frac{\partial W_0}{\partial z} dz = 0 \quad (2.207)$$

$$\int_{-h}^0 \frac{\partial U_0}{\partial x} dz + \int_{-h}^0 \frac{\partial V_0}{\partial y} dz + W_0|_{z=0} - W_0|_{z=-h} = 0 \quad (2.208)$$

$$\int_{-h}^0 \frac{\partial U_0}{\partial x} dz + \int_{-h}^0 \frac{\partial V_0}{\partial y} dz - iN_0 + V_0 \frac{\partial h}{\partial y} \Big|_{z=-h} = 0 \quad (2.209)$$

Note that the height function, h , is a function of y only. So we have

$$\int_{-h}^0 \frac{\partial U_0}{\partial x} dz + \int_{-h}^0 \frac{\partial V_0}{\partial y} dz - iN_0 + V_0 \frac{\partial h}{\partial y} \Big|_{z=-h} = 0. \quad (2.210)$$

We apply the Leibniz integral rule to the first two terms. Note the several terms that result from applying the Leibniz rule result in zero and have been dropped

$$\frac{\partial}{\partial x} \int_{-h}^0 U_0 dz + \frac{\partial}{\partial y} \int_{-h}^0 V_0 dz + V_0 \frac{\partial(-h)}{\partial y} \Big|_{z=-h} - iN_0 + V_0 \frac{\partial h}{\partial y} \Big|_{z=-h} = 0. \quad (2.211)$$

Canceling terms, we have

$$\frac{\partial}{\partial x} \int_{-h}^0 U_0 dz + \frac{\partial}{\partial y} \int_{-h}^0 V_0 dz - iN_0 = 0. \quad (2.212)$$

We integrate over width (from $-\frac{b}{2}$ to $\frac{y'b}{2}$)

$$\int_{-\frac{b}{2}}^{\frac{y'b}{2}} \frac{\partial}{\partial x} \int_{-h}^0 U_0 dz dy + \int_{-\frac{b}{2}}^{\frac{y'b}{2}} \frac{\partial}{\partial y} \int_{-h}^0 V_0 dz dy - \int_{-\frac{b}{2}}^{\frac{y'b}{2}} iN_0 dy = 0 \quad (2.213)$$

$$\int_{-\frac{b}{2}}^{\frac{y'b}{2}} \frac{\partial}{\partial x} \int_{-h}^0 U_0 dz dy + \int_{-h}^0 V_0 dz \Big|_{y=\frac{y'b}{2}} - \int_{-h}^0 V_0 dz \Big|_{y=-\frac{b}{2}} - iN_0 y \Big|_{y=\frac{y'b}{2}} + iN_0 y \Big|_{y=-\frac{b}{2}} = 0 \quad (2.214)$$

We apply the lateral boundary condition

$$\int_{-\frac{b}{2}}^{\frac{y'b}{2}} \frac{\partial}{\partial x} \int_{-h}^0 U_0 dz dy + \int_{-h}^0 V_0 dz \Big|_{y=\frac{y'b}{2}} + \frac{\partial}{\partial x} \left(\frac{b}{2} \right) \int_{-h}^0 U_0 dz \Big|_{y=-\frac{b}{2}} - i \frac{b}{2} y' N_0 - i \frac{b}{2} N_0 = 0. \quad (2.215)$$

We rearrange terms to solve for lateral transport evaluated at $y' \frac{b}{2}$, evaluate the partial derivative of width, b , and substitute the solution for U_0

$$\begin{aligned} \int_{-h}^0 V_0 dz \Big|_{y=\frac{y'b}{2}} &= i \int_{-\frac{b}{2}}^{\frac{y'b}{2}} \frac{\partial}{\partial x} \frac{dN_0}{dx} \int_{-h}^0 \left(1 - \frac{\cosh(\Gamma z)}{\cosh(\Gamma h) + \frac{\Gamma}{\delta} \sinh(\Gamma h)} \right) dz dy \\ - i \mu \frac{b}{2} \frac{dN_0}{dx} \int_{-h}^0 \left(1 - \frac{\cosh(\Gamma z)}{\cosh(\Gamma h) + \frac{\Gamma}{\delta} \sinh(\Gamma h)} \right) dz \Big|_{y=-\frac{b}{2}} &+ i N_0 \frac{b}{2} (y' + 1) \end{aligned} \quad (2.216)$$

We evaluate the integrals over depth, given by P_0 (Eq. (2.145)). Then, we have

$$\int_{-h}^0 V_0 dz \Big|_{y=\frac{y'b}{2}} = i \int_{-\frac{b}{2}}^{\frac{y'b}{2}} \frac{\partial}{\partial x} \frac{dN_0}{dx} P_0 dy - i \mu \frac{b}{2} \frac{dN_0}{dx} P_0 \Big|_{y=-\frac{b}{2}} + i N_0 \frac{b}{2} (y' + 1). \quad (2.217)$$

We apply the Leibniz integral rule again to the first term on the RHS and evaluate the partial derivatives of width, b , with respect to x

$$\begin{aligned} \int_{-h}^0 V_0 dz \Big|_{y=\frac{y'b}{2}} &= i \frac{\partial}{\partial x} \int_{-\frac{b}{2}}^{\frac{y'b}{2}} \frac{dN_0}{dx} P_0 dy - i \frac{dN_0}{dx} P_0 \Big|_{y=\frac{y'b}{2}} \frac{\partial}{\partial x} \left(\frac{y'b}{2} \right) \\ + i \frac{dN_0}{dx} P_0 \Big|_{y=-\frac{b}{2}} \frac{\partial}{\partial x} \left(\frac{-b}{2} \right) &- i \mu \frac{b}{2} \frac{dN_0}{dx} P_0 \Big|_{y=-\frac{b}{2}} + i N_0 \frac{b}{2} (y' + 1) \end{aligned} \quad (2.218)$$

$$\begin{aligned} \int_{-h}^0 V_0 dz \Big|_{y=\frac{y'b}{2}} &= i \frac{\partial}{\partial x} \int_{-\frac{b}{2}}^{\frac{y'b}{2}} \frac{dN_0}{dx} P_0 dy + i \mu y' \frac{b}{2} \frac{dN_0}{dx} P_0 \Big|_{y=\frac{y'b}{2}} \\ + i \mu \frac{b}{2} \frac{dN_0}{dx} P_0 \Big|_{y=-\frac{b}{2}} &- i \mu \frac{b}{2} \frac{dN_0}{dx} P_0 \Big|_{y=-\frac{b}{2}} + i N_0 \frac{b}{2} (y' + 1) \end{aligned} \quad (2.219)$$

Canceling terms, we have

$$\int_{-h}^0 V_0 dz \Big|_{y=\frac{y'b}{2}} = i \frac{\partial}{\partial x} \frac{dN_0}{dx} \int_{-\frac{b}{2}}^{\frac{y'b}{2}} P_0 dy + i \mu y' \frac{b}{2} \frac{dN_0}{dx} P_0 \Big|_{y=\frac{y'b}{2}} + i N_0 \frac{b}{2} (y' + 1). \quad (2.220)$$

Let $y'' = \frac{2y}{b}$. Then, we have

$$\int_{-h}^0 V_0 dz \Big|_{y=\frac{y'b}{2}} = i \frac{\partial}{\partial x} \frac{dN_0}{dx} \frac{b}{2} \int_{-1}^{y'} P_0 dy'' + i \mu y' \frac{b}{2} \frac{dN_0}{dx} P_0 \Big|_{y=\frac{y'b}{2}} + i N_0 \frac{b}{2} (y' + 1). \quad (2.221)$$

Applying the product rule, we obtain

$$\begin{aligned} \int_{-h}^0 V_0 dz \Big|_{y=\frac{y'b}{2}} &= i \left(\frac{b}{2} \frac{d^2 N_0}{dx^2} - \mu \frac{b}{2} \frac{dN_0}{dx} \right) \int_{-1}^{y'} P_0 dy'' \\ &+ i \mu y' \frac{b}{2} \frac{dN_0}{dx} P_0 \Big|_{y=\frac{y'b}{2}} + i N_0 \frac{b}{2} (y' + 1). \end{aligned} \quad (2.222)$$

The solution for V_0 , Eq. (2.205), is integrated over depth, and then will be set equal to Eq. (2.222).

$$\begin{aligned} \int_{-h}^0 V_0 dz &= \frac{f}{\alpha F} \frac{dN_0}{dx} \int_{-h}^0 \left[(1 - p_0) p_h + p_z \right] dz \\ &+ \frac{i\epsilon}{\alpha} \frac{\partial}{\partial y} \left(\frac{1}{h} \int_{-h}^0 \hat{\rho}_1 dz \right) \int_{-h}^0 \left[(1 - p_0) r_h + r_z \right] dz - \frac{i\epsilon}{\alpha^2} \frac{\partial N'}{\partial y} \int_{-h}^0 p_0 dz, \end{aligned} \quad (2.223)$$

which is simplified to

$$\begin{aligned} \int_{-h}^0 V_0 dz &= \frac{f}{\alpha F} \frac{dN_0}{dx} \left[\frac{1}{F} p_h \int_{-h}^0 \cosh(\Gamma z) dz + \int_{-h}^0 p_z dz \right] \\ &+ \frac{i\epsilon}{\alpha} \frac{\partial}{\partial y} \left(\frac{1}{h} \int_{-h}^0 \hat{\rho}_1 dz \right) \left[\frac{1}{F} r_h \int_{-h}^0 \cosh(\Gamma z) dz + \int_{-h}^0 r_z dz \right] \\ &- \frac{i\epsilon}{\alpha^2} \frac{\partial N'}{\partial y} \int_{-h}^0 p_0 dz. \end{aligned} \quad (2.224)$$

The integrals are evaluated and we substitute P_0 , Eq. (2.145), to obtain

$$\begin{aligned} \int_{-h}^0 V_0 dz &= \frac{f}{\alpha F} \frac{dN_0}{dx} \left[\frac{\sinh(\Gamma h)}{\Gamma F} p_h + \int_{-h}^0 p_z dz \right] \\ &+ \frac{i\epsilon}{\alpha} \frac{\partial}{\partial y} \left(\frac{1}{h} \int_{-h}^0 \hat{\rho}_1 dz \right) \left[\frac{\sinh(\Gamma h)}{\Gamma F} r_h + \int_{-h}^0 r_z dz \right] - \frac{i\epsilon}{\alpha^2} \frac{\partial N'}{\partial y} P_0, \end{aligned} \quad (2.225)$$

with $\int_{-h}^0 p_z dz$ and $\int_{-h}^0 r_z dz$ given by

$$\int_{-h}^0 p_z dz = \frac{1}{\Gamma} \sinh(\Gamma h) - \frac{1}{2} \left(h \cosh(\Gamma h) - \frac{1}{\Gamma} \sinh(\Gamma h) \right) - Fh, \quad (2.226)$$

and

$$\int_{-h}^0 r_z dz = \frac{1}{\Gamma^2} \cosh(\Gamma h) - \frac{1}{\Gamma^2} - \frac{h^2}{2}. \quad (2.227)$$

We evaluate Eq. (2.225) at $y = \frac{y'b}{2}$, which is dropped in the equations for ease of writing, and set it equal to Eq. (2.222) to algebraically solve for $\frac{\partial N'}{\partial y}$. First, we move the term with $\frac{\partial N'}{\partial y}$ to one side and move the other terms opposite.

$$\begin{aligned} \frac{i\epsilon}{\alpha^2} \frac{\partial N'}{\partial y} P_0 &= \frac{f}{\alpha F} \frac{dN_0}{dx} \left[\frac{\sinh(\Gamma h)}{F} p_h + \int_{-h}^0 p_z dz \right] + \frac{i\epsilon}{\alpha} \frac{\partial}{\partial y} \left(\frac{1}{h} \int_{-h}^0 \hat{\rho}_1 dz \right) \\ &\quad \left[\frac{\sinh(\Gamma h)}{F} r_h + \int_{-h}^0 r_z dz \right] - i \left(\frac{b}{2} \frac{d^2 N_0}{dx^2} - \mu \frac{b}{2} \frac{dN_0}{dx} \right) \int_{-1}^{y'} P_0 dy'' \\ &\quad - i\mu y' \frac{b}{2} \frac{dN_0}{dx} P_0 - iN_0 \frac{b}{2} (y' + 1). \end{aligned} \quad (2.228)$$

Multiplying both sides by $\frac{-i\alpha^2}{\epsilon P_0}$, the solution for $\frac{\partial N'}{\partial y}$ is obtained, given by

$$\begin{aligned} \frac{\partial N'}{\partial y} &= -\frac{if\alpha}{\epsilon F} \frac{1}{P_0} \left[\frac{\sinh(\Gamma h)}{F} p_h + \int_{-h}^0 p_z dz \right] \frac{dN_0}{dx} + \alpha \frac{1}{P_0} \frac{\partial}{\partial y} \left(\frac{1}{h} \int_{-h}^0 \hat{\rho}_1 dz \right) \\ &\quad \left[\frac{\sinh(\Gamma h)}{F} r_h + \int_{-h}^0 r_z dz \right] - \frac{\alpha^2}{\epsilon} \frac{1}{P_0} \left(\frac{b}{2} \frac{d^2 N_0}{dx^2} - \mu \frac{b}{2} \frac{dN_0}{dx} \right) \int_{-1}^{y'} P_0 dy'' \\ &\quad - \frac{\alpha^2}{\epsilon} \mu y' \frac{b}{2} \frac{dN_0}{dx} - N_0 \frac{1}{P_0} \frac{b\alpha^2}{2\epsilon} (y' + 1). \end{aligned} \quad (2.229)$$

We now solve for the lateral gradient of the depth mean density:

$$\frac{\partial}{\partial y} \left(\frac{1}{h} \int_{-h}^0 \hat{\rho}_1 dz \right),$$

which is the final component needed for V_0 . Recall the zero order density balance equation and respective boundary condition at the surface and bottom are given by

$$-i\hat{\rho}_1 + U_0 \frac{d\rho_0}{dx} = \frac{K_v}{2} \frac{\partial^2 \hat{\rho}_1}{\partial z^2}, \quad (2.230)$$

and

$$\frac{\partial \hat{\rho}_1}{\partial z} = 0. \quad (2.231)$$

We first integrate Eq. (2.230) over depth to obtain

$$-i \int_{-h}^0 \hat{\rho}_1 dz + \frac{d\rho_0}{dx} \int_{-h}^0 U_0 dz = \int_{-h}^0 \frac{K_v}{2} \frac{\partial^2 \hat{\rho}_1}{\partial z^2} dz. \quad (2.232)$$

We evaluate the integral on the RHS and apply the boundary condition, Eq. (2.231).

$$-i \int_{-h}^0 \hat{\rho}_1 dz + \frac{d\rho_0}{dx} \int_{-h}^0 U_0 dz = 0. \quad (2.233)$$

We rearrange terms and integrate Eq. (2.137) over depth, substituting (??), to obtain

$$-i \int_{-h}^0 \hat{\rho}_1 dz = i \frac{dN_0}{dx} \frac{d\rho_0}{dx} P_0. \quad (2.234)$$

Next, we multiply both sides by $\frac{i}{h}$:

$$\frac{1}{h} \int_{-h}^0 \hat{\rho}_1 dz = -\frac{1}{h} \frac{dN_0}{dx} \frac{d\rho_0}{dx} P_0. \quad (2.235)$$

For the lateral gradient, we take the partial derivative with respect to y :

$$\frac{\partial}{\partial y} \left(\frac{1}{h} \int_{-h}^0 \hat{\rho}_1 dz \right) = -\frac{dN_0}{dx} \frac{d\rho_0}{dx} \frac{\partial}{\partial y} \left(\frac{1}{h} P_0 \right). \quad (2.236)$$

In the following two steps, we first apply the product rule and then the chain rule to evaluate $\frac{\partial}{\partial y} \left(\frac{1}{h} P_0 \right)$:

$$\frac{\partial}{\partial y} \left(\frac{1}{h} \int_{-h}^0 \hat{\rho}_1 dz \right) = -\frac{dN_0}{dx} \frac{d\rho_0}{dx} \left(P_0 \frac{\partial}{\partial y} \left(\frac{1}{h} \right) + \frac{1}{h} \frac{\partial P_0}{\partial y} \right), \quad (2.237)$$

$$\frac{\partial}{\partial y} \left(\frac{1}{h} \int_{-h}^0 \hat{\rho}_1 dz \right) = -\frac{dN_0}{dx} \frac{d\rho_0}{dx} \left(-\frac{1}{h^2} P_0 \frac{\partial h}{\partial y} + \frac{1}{h} \frac{\partial P_0}{\partial h} \frac{\partial h}{\partial y} \right). \quad (2.238)$$

We simplify to obtain the lateral gradient of the depth mean density

$$\frac{\partial}{\partial y} \left(\frac{1}{h} \int_{-h}^0 \hat{\rho}_1 dz \right) = -\frac{dN_0}{dx} \frac{d\rho_0}{dx} \frac{1}{h} \frac{\partial h}{\partial y} \left(\frac{\partial P_0}{\partial h} - \frac{1}{h} P_0 \right). \quad (2.239)$$

2.1.4.4 Vertical Velocity

To solve for W_0 , we integrate the continuity equation, Eq. (2.110), from $-h$ to z and apply the partial slip boundary condition, Eq. (2.119),

$$\int_{-h}^z \frac{\partial U_0}{\partial x} dz + \int_{-h}^z \frac{\partial V_0}{\partial y} dz + W_0|_z - W_0|_{-h} = 0. \quad (2.240)$$

We rearrange terms, to solve for W_0 at z , and apply the partial slip boundary condition, Eq. (2.119), to obtain

$$W_0|_z = - \int_{-h}^z \frac{\partial U_0}{\partial x} dz - \int_{-h}^z \frac{\partial V_0}{\partial y} dz - V_0 \frac{\partial h}{\partial y}. \quad (2.241)$$

The partial of U_0 , Eq. (2.137), with respect to x is given by

$$\frac{\partial U_0}{\partial x} = -i \frac{d^2 N_0}{dx^2} \left(1 - \frac{\cosh(\Gamma z)}{\cosh(\Gamma h) + \frac{\Gamma}{\delta} \sinh(\Gamma h)} \right). \quad (2.242)$$

Integrating over depth, we have

$$\int_{-h}^z \frac{\partial U_0}{\partial x} dz = -i \frac{d^2 N_0}{dx^2} \left(z + h - \frac{\sinh(\Gamma z) + \sinh(\Gamma h)}{\Gamma (\cosh(\Gamma h) + \frac{\Gamma}{\delta} \sinh(\Gamma h))} \right). \quad (2.243)$$

Next, we take the partial derivative of V_0 with respect to y

$$\begin{aligned} \frac{\partial V_0}{\partial y} &= \frac{f}{\alpha} \left[\frac{-2 \cosh(\Gamma z)}{F^3} \frac{\partial F}{\partial y} p_h + \frac{\cosh(\Gamma z)}{F^2} \frac{\partial p_h}{\partial y} \right. \\ &+ \left. \frac{-1}{F^2} \frac{\partial F}{\partial y} p_z + \frac{1}{F} \frac{\partial p_z}{\partial y} \right] \frac{dN_0}{dx} \\ &+ \frac{i\epsilon}{\alpha} \left[\left(-\frac{\cosh(\Gamma z)}{F^2} \frac{\partial F}{\partial y} r_h + \frac{\cosh(\Gamma z)}{F} \frac{\partial r_h}{\partial y} \right) \frac{\partial}{\partial y} \left(\frac{1}{h} \int_{-h}^0 \hat{\rho}_1 dz \right) \right. \\ &+ \left. \left(\frac{\cosh(\Gamma z)}{F} r_h + r_z \right) \frac{\partial^2}{\partial y^2} \left(\frac{1}{h} \int_{-h}^0 \hat{\rho}_1 dz \right) \right] \\ &+ \frac{i\epsilon}{\alpha^2} \left[-\frac{\cosh(\Gamma z)}{F^2} \frac{\partial F}{\partial y} \frac{\partial N'}{\partial y} + \left(\frac{\cosh(\Gamma z)}{F} - 1 \right) \frac{\partial^2 N'}{\partial y^2} \right], \end{aligned} \quad (2.244)$$

with the partial derivatives given by

$$\begin{aligned}
\frac{\partial F}{\partial y} &= \left(\Gamma \sinh(\Gamma h) + \frac{\Gamma^2}{\delta} \cosh(\Gamma h) \right) \frac{\partial h}{\partial y} \\
\frac{\partial p_h}{\partial y} &= \frac{\partial F}{\partial y} + \left(\Gamma \cosh(\Gamma h) \left(\frac{\Gamma h}{2} - \frac{\Gamma}{2\delta} \right) + \frac{\Gamma}{2} \sinh(\Gamma h) \right. \\
&\quad \left. + \Gamma \sinh(\Gamma h) \left(\frac{\Gamma^2 h}{2\delta} - 1 \right) + \frac{\Gamma^2}{2\delta} \cosh(\Gamma h) \right) \frac{\partial h}{\partial y} \\
\frac{\partial p_z}{\partial y} &= \frac{\partial F}{\partial y} \\
\frac{\partial r_h}{\partial y} &= \left(-F + 1 \right) \frac{\partial h}{\partial y}.
\end{aligned} \tag{2.245}$$

The derivative with respect to y of the lateral gradient of the depth mean density, Eq.

(2.239), is given by

$$\begin{aligned}
\frac{\partial^2}{\partial y^2} \left(\frac{1}{h} \int_{-h}^0 \hat{\rho}_1 dz \right) &= -\frac{dN_0}{dx} \frac{d\rho_0}{dx} \left[\frac{1}{h^2} \left(\frac{\partial h}{\partial y} \right)^2 \left(\frac{1}{h} P_0 - \frac{\partial P_0}{\partial h} \right) \right. \\
&\quad \left. + \frac{1}{h} \frac{\partial^2 h}{\partial y^2} \left(\frac{\partial P_0}{\partial h} - \frac{1}{h} P_0 \right) + \frac{1}{h} \frac{\partial h}{\partial y} \left(\frac{\partial^2 P_0}{\partial h^2} \frac{\partial h}{\partial y} + \frac{1}{h^2} \frac{\partial h}{\partial y} - \frac{1}{h} \frac{\partial P_0}{\partial h} \frac{\partial h}{\partial y} \right) \right].
\end{aligned} \tag{2.246}$$

The second derivative of the higher order sea level with respect to y is given by

$$\begin{aligned}
\frac{\partial^2 N'}{\partial y^2} &= \frac{if\alpha}{\epsilon} \left[\frac{2}{F^3} \frac{\partial F}{\partial y} \frac{1}{P_0} \frac{\sinh(\Gamma h)}{\Gamma} p_h + \frac{1}{F^2} \frac{\partial}{\partial y} \left(\frac{-1}{P_0} \right) \frac{\sinh(\Gamma h)}{\Gamma} p_h \right. \\
&\quad - \frac{1}{F^2} \frac{1}{P_0} \cosh(\Gamma h) p_h - \frac{1}{F^2} \frac{1}{P_0} \frac{\sinh(\Gamma h)}{\Gamma} \frac{\partial p_h}{\partial y} + \frac{1}{F^2} \frac{\partial F}{\partial y} \frac{1}{P_0} P_z \\
&\quad - \frac{1}{F} P_z \frac{\partial}{\partial y} \frac{1}{P_0} - \frac{1}{F} \frac{1}{P_0} \frac{\partial P_z}{\partial y} \left. \right] \frac{dN_0}{dx} - \alpha \left[\left(- \left((h - P_0) r_h + R_z \right) \frac{\partial}{\partial y} \frac{1}{P_0} \right. \right. \\
&\quad - \frac{1}{P_0} \left(\frac{\partial}{\partial y} \left((h - P_0) r_h + (h - P_0) \frac{\partial r_h}{\partial y} + \frac{\partial R_z}{\partial y} \right) \frac{\partial}{\partial y} \left(\frac{1}{h} \int_{-h}^0 \hat{\rho}_1 dz \right) \right. \\
&\quad \left. \left. - \frac{1}{P_0} \left((h - P_0) r_h + R_z \right) \frac{\partial^2}{\partial y^2} \left(\frac{1}{h} \int_{-h}^0 \hat{\rho}_1 dz \right) \right] \right. \\
&\quad \left. \frac{b\alpha^2}{2\epsilon} \left[- \frac{\partial}{\partial y} \frac{1}{P_0} \left(\left(\frac{d^2 N_0}{dx^2} - \mu \frac{dN_0}{dx} \right) \int_{-1}^{y'} P_0 dy'' + \mu y' \frac{dN_0}{dx} P_0 + N_0 (y' + 1) \right) \right. \right. \\
&\quad - \frac{1}{P_0} \left(\left(\frac{d^2 N_0}{dx^2} - \mu \frac{dN_0}{dx} \right) \frac{\partial}{\partial y} \int_{-1}^{y'} P_0 dy'' \right. \\
&\quad \left. \left. + \mu N_0 \left(\frac{2}{b} P_0 + \frac{\partial P_0}{\partial y} y' \right) + \frac{2N_0}{b} \right] \right],
\end{aligned} \tag{2.247}$$

with partial derivatives given by

$$\begin{aligned}
-\frac{\partial}{\partial y} \frac{1}{P_0} &= \frac{1}{\left(\frac{\sinh(\Gamma h)}{\Gamma F} - h\right)^2} \left(\frac{\Gamma^2 F \cosh(\Gamma h) - \Gamma \frac{\partial F}{\partial h} \sinh(\Gamma h)}{\Gamma^2 F^2} - 1 \right) \frac{\partial h}{\partial y} \\
\frac{\partial P_z}{\partial y} &= - \left(\frac{\partial F}{\partial y} + F \frac{\partial h}{\partial y} \right) \\
&- \frac{1}{2} \left(\Gamma h \sinh(\Gamma h) + \cosh(\Gamma h) \right) \frac{\partial h}{\partial y} + \frac{3 \cosh(\Gamma h)}{2} \frac{\partial h}{\partial y} \\
\frac{\partial R_z}{\partial y} &= \left(\frac{\sinh(\Gamma h)}{\Gamma} - h \right) \frac{\partial h}{\partial y}.
\end{aligned} \tag{2.248}$$

We integrate the partial derivative of V_0 with respect to y from $-h$ to z :

$$\begin{aligned}
\int_{-h}^z \frac{\partial V_0}{\partial y} dz &= \frac{f}{\alpha} \frac{dN_0}{dx} \left[- \frac{2}{F^3} \frac{\partial F}{\partial y} p_h \int_{-h}^z \cosh(\Gamma z) dz + \frac{1}{F^2} \frac{\partial p_h}{\partial y} \int_{-h}^z \cosh(\Gamma z) dz \right. \\
&- \left. \frac{1}{F^2} \frac{\partial F}{\partial y} \int_{-h}^z p_z dz + \frac{1}{F} \frac{\partial p_z}{\partial y} \int_{-h}^z dz \right] + \frac{i\epsilon}{\alpha} \left[\frac{\partial}{\partial y} \left(\frac{1}{h} \int_{-h}^0 \hat{\rho}_1 dz \right) \right. \\
&\left(- \frac{1}{F^2} \frac{\partial F}{\partial y} r_h \int_{-h}^z \cosh(\Gamma z) dz + \frac{1}{F} \frac{\partial r_h}{\partial y} \int_{-h}^z \cosh(\Gamma z) dz \right) \\
&+ \frac{\partial^2}{\partial y^2} \left(\frac{1}{h} \int_{-h}^0 \hat{\rho}_1 dz \right) \left(\frac{1}{F} r_h \int_{-h}^z \cosh(\Gamma z) dz + \int_{-h}^z r_z dz \right) \Big] \\
&+ \frac{i\epsilon}{\alpha^2} \left[- \frac{\partial N'}{\partial y} \frac{1}{F^2} \frac{\partial F}{\partial y} \int_{-h}^z \cosh(\Gamma z) dz \right. \\
&+ \left. \frac{\partial^2 N'}{\partial y^2} \int_{-h}^z \left(\frac{\cosh(\Gamma z)}{F} - 1 \right) dz \right].
\end{aligned} \tag{2.249}$$

We evaluate the integrals to obtain

$$\begin{aligned}
\int_{-h}^z \frac{\partial V_0}{\partial y} dz &= \frac{f dN_0}{\alpha dx} \left[-\frac{2}{\Gamma F^3} \frac{\partial F}{\partial y} p_h \left(\sinh(\Gamma z) - \sinh(-\Gamma h) \right) + \frac{1}{\Gamma F^2} \frac{\partial p_h}{\partial y} \right. \\
&\quad \left(\sinh(\Gamma z) - \sinh(-\Gamma h) \right) - \frac{1}{F^2} \frac{\partial F}{\partial y} \int_{-h}^z p_z dz + \frac{1}{F} \frac{\partial p_z}{\partial y} (z + h) \Big] \\
&+ \frac{i\epsilon}{\alpha} \left[\frac{\partial}{\partial y} \left(\frac{1}{h} \int_{-h}^0 \hat{\rho}_1 dz \right) \left(-\frac{1}{\Gamma F^2} \frac{\partial F}{\partial y} r_h \left(\sinh(\Gamma z) - \sinh(-\Gamma h) \right) \right. \right. \\
&+ \left. \left. \frac{1}{\Gamma F} \frac{\partial r_h}{\partial y} \left(\sinh(\Gamma z) - \sinh(-\Gamma h) \right) \right) \right] + \frac{\partial^2}{\partial y^2} \left(\frac{1}{h} \int_{-h}^0 \hat{\rho}_1 dz \right) \tag{2.250} \\
&\left(\frac{1}{\Gamma F} r_h \left(\sinh(\Gamma z) - \sinh(-\Gamma h) \right) \right. \\
&+ \left. \int_{-h}^z r_z dz \right) \Big] \\
&+ \frac{i\epsilon}{\alpha^2} \left[-\frac{\partial N'}{\partial y} \frac{1}{\Gamma F^2} \frac{\partial F}{\partial y} \left(\sinh(\Gamma z) - \sinh(-\Gamma h) \right) \right. \\
&+ \left. \frac{\partial^2 N'}{\partial y^2} \left(\frac{\sinh(\Gamma z) - \sinh(-\Gamma h)}{\Gamma F} - (z + h) \right) \right].
\end{aligned}$$

We substitute $\sinh(-\Gamma h) = -\sinh(\Gamma h)$:

$$\begin{aligned}
\int_{-h}^z \frac{\partial V_0}{\partial y} dz &= \frac{f dN_0}{\alpha dx} \left[-\frac{2}{\Gamma F^3} \frac{\partial F}{\partial y} p_h \left(\sinh(\Gamma z) + \sinh(\Gamma h) \right) \right. \\
&+ \frac{1}{\Gamma F^2} \frac{\partial p_h}{\partial y} \left(\sinh(\Gamma z) + \sinh(\Gamma h) \right) \\
&- \left. \frac{1}{F^2} \frac{\partial F}{\partial y} \int_{-h}^z p_z dz + \frac{1}{F} \frac{\partial p_z}{\partial y} (z + h) \right] \\
&+ \frac{i\epsilon}{\alpha} \left[\frac{\partial}{\partial y} \left(\frac{1}{h} \int_{-h}^0 \hat{\rho}_1 dz \right) \left(-\frac{1}{\Gamma F^2} \frac{\partial F}{\partial y} r_h \left(\sinh(\Gamma z) + \sinh(\Gamma h) \right) \right) \right. \\
&+ \left. \frac{1}{\Gamma F} \frac{\partial r_h}{\partial y} \left(\sinh(\Gamma z) + \sinh(\Gamma h) \right) \right) \\
&+ \left. \frac{\partial^2}{\partial y^2} \left(\frac{1}{h} \int_{-h}^0 \hat{\rho}_1 dz \right) \left(\frac{1}{\Gamma F} r_h \left(\sinh(\Gamma z) + \sinh(\Gamma h) \right) + \int_{-h}^z r_z dz \right) \right] \\
&+ \frac{i\epsilon}{\alpha^2} \left[-\frac{\partial N'}{\partial y} \frac{1}{\Gamma F^2} \frac{\partial F}{\partial y} \left(\sinh(\Gamma z) + \sinh(\Gamma h) \right) \right. \\
&+ \left. \frac{\partial^2 N'}{\partial y^2} \left(\frac{\sinh(\Gamma z) + \sinh(\Gamma h)}{\Gamma F} - (z + h) \right) \right], \tag{2.251}
\end{aligned}$$

where the integrals over depth of p_z and r_z , Eqs. (2.202) and (2.204), respectively, are given by

$$\begin{aligned}
\int_{-h}^z p_z dz &= \frac{1}{\Gamma} \left(\sinh(\Gamma z) + \sinh(\Gamma h) \right) - \frac{1}{2} \left(z \cosh(\Gamma z) + h \cosh(\Gamma h) \right. \\
&- \left. \frac{1}{\Gamma} \left(\sinh(\Gamma z) + \sinh(\Gamma h) \right) \right) - F(z + h) \tag{2.252}
\end{aligned}$$

and

$$\int_{-h}^z r_z dz = -\frac{1}{\Gamma^2} \left(\cosh(\Gamma z) - \cosh(\Gamma h) \right) + \frac{z^2 - h^2}{2}. \tag{2.253}$$

The final solution for W_0 , Eq. (2.241), is found by combining negative Eq. (2.243), negative Eq. (2.251), and the negative product of Eq. (2.205) and the partial derivative of

h with respect to y . Thus, W_0 is given by

$$\begin{aligned}
W_0 = & i \frac{d^2 N_0}{dx^2} \left(z + h - \frac{\sinh(\Gamma z) + \sinh(\Gamma h)}{\Gamma F} \right) \\
& - \frac{f}{\alpha} \frac{dN_0}{dx} \left[- \frac{2}{\Gamma F^3} \frac{\partial F}{\partial y} p_h \left(\sinh(\Gamma z) + \sinh(\Gamma h) \right) \right. \\
& + \frac{1}{\Gamma F^2} \frac{\partial p_h}{\partial y} \left(\sinh(\Gamma z) + \sinh(\Gamma h) \right) - \frac{1}{F^2} \frac{\partial F}{\partial y} \int_{-h}^z p_z dz \\
& + \left. \frac{1}{F} \frac{\partial p_z}{\partial y} (z + h) \right] - \frac{i\epsilon}{\alpha} \left[\frac{\partial}{\partial y} \left(\frac{1}{h} \int_{-h}^0 \hat{\rho}_1 dz \right) \left(- \frac{1}{\Gamma F^2} \frac{\partial F}{\partial y} r_h \right. \right. \\
& \left. \left. \left(\sinh(\Gamma z) + \sinh(\Gamma h) \right) + \frac{1}{\Gamma F} \frac{\partial r_h}{\partial y} \left(\sinh(\Gamma z) + \sinh(\Gamma h) \right) \right) \right. \\
& \left. + \frac{\partial^2}{\partial y^2} \left(\frac{1}{h} \int_{-h}^0 \hat{\rho}_1 dz \right) \left(\frac{1}{\Gamma F} r_h \left(\sinh(\Gamma z) + \sinh(\Gamma h) \right) + \int_{-h}^z r_z dz \right) \right] \\
& - \frac{i\epsilon}{\alpha^2} \left[- \frac{\partial N'}{\partial y} \frac{1}{\Gamma F^2} \frac{\partial F}{\partial y} \left(\sinh(\Gamma z) + \sinh(\Gamma h) \right) \right. \\
& \left. + \frac{\partial^2 N'}{\partial y^2} \left(\frac{\sinh(\Gamma z) + \sinh(\Gamma h)}{\Gamma F} - (z + h) \right) \right] \\
& - \left(\frac{f}{\alpha F} \left[(1 - p_0) p_h + p_z \right] \frac{dN_0}{dx} + \frac{i\epsilon}{\alpha} \left[(1 - p_0) r_h + r_z \right] \frac{\partial}{\partial y} \left(\frac{1}{h} \int_{-h}^0 \hat{\rho}_1 dz \right) \right. \\
& \left. - \frac{i\epsilon}{\alpha^2} p_0 \frac{\partial N'}{\partial y} \right) \frac{\partial h}{\partial y}.
\end{aligned} \tag{2.254}$$

CHAPTER 3

RESULTS AND DISCUSSION

In this chapter, the results are presented and discussed. First, the analytical model is summarized, in addition to a brief discussion of the study area. The model is derived from the zero-order solution of a perturbation expansion about $\epsilon = \frac{A_{M2}}{h_{max}}$ of the Navier-Stokes equations. Recall, the zero-order expansion represents the tidal flow, while the first-order expansion represents the residual flow within the estuary. The first-order expansion, thus residual flow, is not considered in this paper. Furthermore, non-linear terms which create asymmetric tides are excluded from the governing equations and vertical eddy viscosity is assumed to be constant. Estuary width, $b(x)$ and estuary depth, $h(y)$, are given by

$$\begin{aligned} b(x) &= e^{-\mu x}, \\ h(y) &= \epsilon + (1 - \epsilon)(1 - y^2). \end{aligned} \tag{3.1}$$

Water level elevation, $\eta(t, x)$ is given by

$$\eta_0(t, x) = Re \left(\left(\frac{\frac{\mu}{2} \sin(d_0(l-x)) + d_0 \cos(d_0(l-x))}{\frac{\mu}{2} \sin(d_0 l) + d_0 \cos(d_0 l)} \right) e^{\frac{\mu x}{2} - it} \right). \tag{3.2}$$

Along-channel velocity, $u(t, x, y, z)$, and across-channel velocity are given by

$$u_0(t, x, y, z) = Re \left(-i \frac{dN_0}{dx} p_0 e^{-it} \right), \tag{3.3}$$

and

$$\begin{aligned} v_0(t, x, y, z) &= Re \left(\left(\frac{f}{\alpha F} \left[(1 - p_0) p_h + p_z \right] \frac{dN_0}{dx} \right. \right. \\ &\quad \left. \left. + \frac{i\epsilon}{\alpha} \left[(1 - p_0) r_h + r_z \right] \frac{\partial}{\partial y} \left(\frac{1}{h} \int_{-h}^0 \hat{\rho}_1 dz \right) - \right. \right. \\ &\quad \left. \left. \frac{i\epsilon}{\alpha^2} p_0 \frac{\partial N'}{\partial y} \right) e^{-it} \right), \end{aligned} \tag{3.4}$$

with the identities

$$\begin{aligned}
F &= \cosh(\Gamma h) + \frac{\Gamma}{\delta} \sinh(\Gamma h), \\
p_0 &= 1 - \frac{\cosh(\Gamma z)}{\frac{\Gamma}{\delta} \sinh(\Gamma h) + \cosh(\Gamma h)}, \\
p_h &= F + \sinh(\Gamma h) \left(\frac{\Gamma h}{2} - \frac{\Gamma}{2\delta} \right) + \cosh(\Gamma h) \left(\frac{\Gamma^2}{2\delta} - 1 \right), \\
p_z &= \cosh(\Gamma z) - \frac{\Gamma z}{2} \sinh(\Gamma z) - F, \\
r_h &= -\frac{1}{\Gamma} \sinh(\Gamma h) - \frac{1}{\delta} \cosh(\Gamma h) + h + \frac{1}{\delta}, \\
r_z &= -\frac{1}{\Gamma} \sinh(\Gamma z) + z.
\end{aligned} \tag{3.5}$$

and the along-channel gradient of the water level magnitude, N_0 , is

$$\begin{aligned}
\frac{dN_0}{dx} &= \frac{\mu}{2} e^{\frac{\mu x}{2}} \left(\frac{\frac{\mu}{2} \sin(d_0(l-x)) + d_0 \cos(d_0(l-x))}{\frac{\mu}{2} \sin(d_0 l) + d_0 \cos(d_0 l)} \right) \\
&+ e^{\frac{\mu x}{2}} \left(\frac{d_0^2 \sin(d_0(l-x)) - \frac{d_0 \mu}{2} \cos(d_0(l-x))}{\frac{\mu}{2} \sin(d_0 l) + d_0 \cos(d_0 l)} \right).
\end{aligned} \tag{3.6}$$

The lateral gradient of higher order sea level, N' , is given by

$$\begin{aligned}
\frac{\partial N'}{\partial y} &= -\frac{if\alpha}{\epsilon F} \frac{1}{P_0} \left[\frac{\sinh(\Gamma h)}{F} p_h + \int_{-h}^0 p_z dz \right] \frac{dN_0}{dx} + \alpha \frac{1}{P_0} \frac{\partial}{\partial y} \left(\frac{1}{h} \int_{-h}^0 \hat{\rho}_1 dz \right) \\
&\left[\frac{\sinh(\Gamma h)}{F} r_h + \int_{-h}^0 r_z dz \right] - \frac{\alpha^2}{\epsilon} \frac{1}{P_0} \left(\frac{b}{2} \frac{d^2 N_0}{dx^2} - \mu \frac{b}{2} \frac{dN_0}{dx} \right) \int_{-1}^{y'} P_0 dy'' \\
&- \frac{\alpha^2}{\epsilon} \mu y' \frac{b}{2} \frac{dN_0}{dx} - N_0 \frac{1}{P_0} \frac{b\alpha^2}{2\epsilon} (y' + 1),
\end{aligned} \tag{3.7}$$

and the lateral gradient of the depth mean density is given by

$$\frac{\partial}{\partial y} \left(\frac{1}{h} \int_{-h}^0 \hat{\rho}_1 dz \right) = -\frac{dN_0}{dx} \frac{d\rho_0}{dx} \frac{1}{h} \frac{\partial h}{\partial y} \left(\frac{\partial P_0}{\partial h} - \frac{1}{h} P_0 \right). \tag{3.8}$$

Vertical velocity, $w(t, x, y, z)$, is given by

$$\begin{aligned}
w_0(t, x, y, z) = & Re \left(\left[i \frac{d^2 N_0}{dx^2} \left(z + h - \frac{\sinh(\Gamma z) + \sinh(\Gamma h)}{\Gamma F} \right) \right. \right. \\
& - \frac{f}{\alpha} \frac{dN_0}{dx} \left[- \frac{2}{\Gamma F^3} \frac{\partial F}{\partial y} p_h \left(\sinh(\Gamma z) + \sinh(\Gamma h) \right) \right. \\
& + \frac{1}{\Gamma F^2} \frac{\partial p_h}{\partial y} \left(\sinh(\Gamma z) + \sinh(\Gamma h) \right) - \frac{1}{F^2} \frac{\partial F}{\partial y} \int_{-h}^z p_z dz \\
& + \left. \left. \frac{1}{F} \frac{\partial p_z}{\partial y} (z + h) \right] - \frac{i\epsilon}{\alpha} \left[\frac{\partial}{\partial y} \left(\frac{1}{h} \int_{-h}^0 \hat{\rho}_1 dz \right) \left(- \frac{1}{\Gamma F^2} \frac{\partial F}{\partial y} r_h \right. \right. \right. \\
& \left. \left. \left(\sinh(\Gamma z) + \sinh(\Gamma h) \right) + \frac{1}{\Gamma F} \frac{\partial r_h}{\partial y} \left(\sinh(\Gamma z) + \sinh(\Gamma h) \right) \right) \right) \\
& + \frac{\partial^2}{\partial y^2} \left(\frac{1}{h} \int_{-h}^0 \hat{\rho}_1 dz \right) \left(\frac{1}{\Gamma F} r_h \left(\sinh(\Gamma z) + \sinh(\Gamma h) \right) \right. \\
& \left. + \int_{-h}^z r_z dz \right] - \frac{i\epsilon}{\alpha^2} \left[- \frac{\partial N'}{\partial y} \frac{1}{\Gamma F^2} \frac{\partial F}{\partial y} \left(\sinh(\Gamma z) + \sinh(\Gamma h) \right) \right. \\
& + \left. \left. \frac{\partial^2 N'}{\partial y^2} \left(\frac{\sinh(\Gamma z) + \sinh(\Gamma h)}{\Gamma F} - (z + h) \right) \right] \right. \\
& - \left. \left(\frac{f}{\alpha F} \left[(1 - p_0) p_h + p_z \right] \frac{dN_0}{dx} \right. \right. \\
& \left. \left. + \frac{i\epsilon}{\alpha} \left[(1 - p_0) r_h + r_z \right] \frac{\partial}{\partial y} \left(\frac{1}{h} \int_{-h}^0 \hat{\rho}_1 dz \right) - \frac{i\epsilon}{\alpha^2 p_0} \frac{\partial N'}{\partial y} \right) \frac{\partial h}{\partial y} \right] e^{-it}.
\end{aligned} \tag{3.9}$$

The model is applied to study tidal flow dynamics of the Damariscotta River estuary (DRE) using Matlab software. Figure 3.1 shows the estuary from above and its location in Maine. The estuary is tidally-dominated and weakly-stratified. It is relatively short, with length of 30.6 km, and narrow. The width converges from 963 m at the mouth to 45 m at the head. The tides are semi-diurnal dominant with a period of 12.42 h. Tidal amplitude ranges from 0.8 to 2.1 m between neap and spring tides [7].



Figure 3.1. Location and satellite (Google Earth) image of the study area: the Damariscotta River Estuary, ME. Location and satellite (Google Earth) image of the study area: the Damariscotta River estuary, ME.

The results of the model will be presented and discussed for water elevation, along-channel and across-channel velocity in the context of previous studies. First, the variation of water elevation amplitude and phase along the length of the estuary is considered. Next, along channel velocity amplitude and phase at one location in the cross-section of the estuary is examined for the entire distance along the estuary. This leads to an investigation into three-dimensional variations of the amplitude and phase of the along-channel velocity. Then, variations over the tidal cycle in three-dimensional velocity, particularly the along- and across-channel velocities, are examined. Vertical eddy viscosity, A_v , and the width convergence factor, μ , are then varied independently to study sensitivity to changes in friction and width convergence of water level and along-channel velocity. Lastly, the limitations of the model are discussed in addition to suggestions for future work.

3.1 Water Elevation

Along-channel variations in water elevation, η , within the Damariscotta River Estuary are first investigated. Due to the narrow width of the estuary, the zero-order water level does not vary across the channel. Thus, amplitude of water elevation is a function of only along-channel distance into the estuary, x . Figure 3.2 shows the amplitude and phase of water elevation of the Damariscotta estuary as a function of along-channel position.

Towards the head, tidal amplitude increases from 1.5 m to 3 m, indicative of tidal amplification due to width convergence. Lieberthal et al. (2019) considers overtides, due to the D2, D4, and D6 tidal constituents, which are found to be amplified in the estuary. The phase of η increases to approximately 60 degrees at the head of the estuary (Fig. 3.2). This is interpreted as a time lag of about two hours in water elevation between the mouth and head of the estuary.

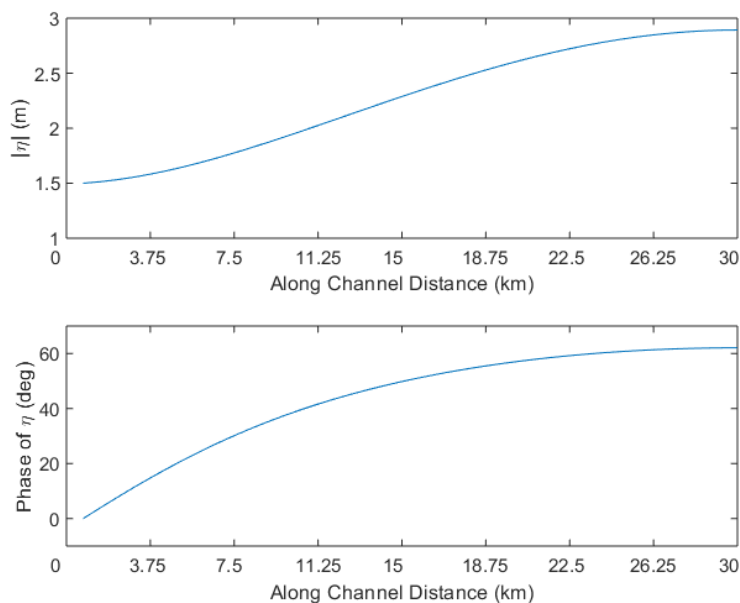


Figure 3.2. Amplitude and phase of water level elevation (η) as a function of along-channel distance into the estuary, x .

3.2 Velocity

Tidal flow velocity within the Damariscotta estuary is examined in this section, focusing first on the along-channel component, u , and then the lateral and vertical components, v and w respectively. In Figure 3.3, amplitude and phase of along-channel velocity at the center and surface of the channel are shown as a function of along-channel position in the estuary. Amplitude of along-channel velocity near the surface, center of the channel ranges from approximately 0.2 to 0.4 m/s within the estuary. This compares well with Lieberthal et al. (2019) which found maximum along-channel velocity amplitude of 0.4 m/s predicted in a perturbation model of the Damariscotta estuary. Along-channel velocity amplitude increases slightly at first, but decreases from the mouth towards the head due to friction. This is notable because water level amplitude shows an increase with along-channel distance. The result suggests that width convergence is more important in determining water level elevation while friction has stronger influence on along-channel velocity, which is evident in the solution for U_0 . This makes it difficult to determine which, convergence or friction, is more important to estuary dynamics. The Damariscotta estuary cannot be classified as hypersynchronous or hyposynchronous based on definitions in Chapter 1. The following section will examine the influences of friction and convergence further.

Phase of along-channel velocity, u , increases along the estuary from 78 to 88 deg, which is a slight increase of 10 deg or 0.3 h, until just after mid-estuary (Fig. 3.3). At about 18 km into the estuary, phase sharply decreases towards the head of the estuary by about 30 deg or 1 h. Unfortunately, along-channel variations in along-channel velocity phase difference are not presented in Lieberthal et al. (2019) for comparison.

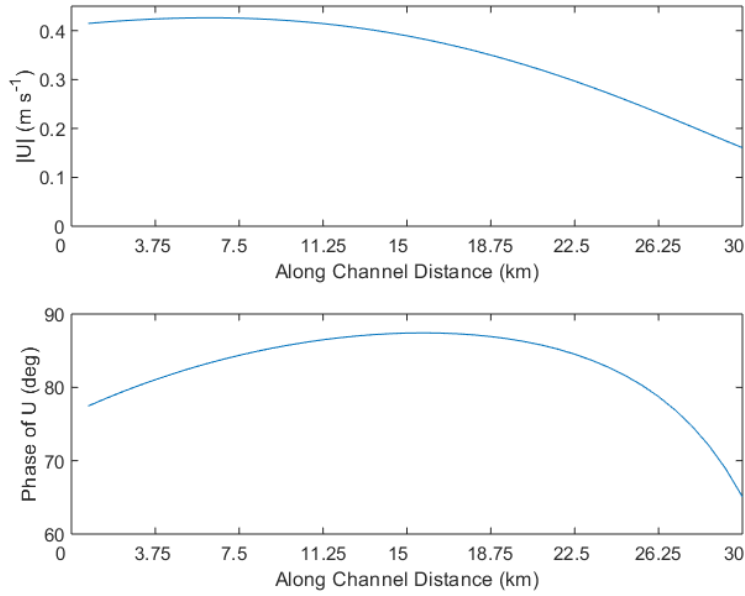


Figure 3.3. Amplitude and phase of along-channel velocity, u , at the center, surface of the channel as a function of distance along the estuary, x .

It is important to note that along-channel velocity varies within the estuary cross-section and Fig. 3.3 is for a single location within the cross-section. This leads to a necessary investigation into three-dimensional variability of the amplitude and phase of along-channel velocity, as shown in Figure 3.4. Along-channel velocity amplitude diminishes towards the bottom of the estuary and towards the sides of the channel due to increased friction near the boundary of the channel (Fig. 3.4a,c,e). This matches well with results of previous work within the Damariscotta estuary [4, 7]. Phase of along channel velocity increases from -100 deg at the lateral boundaries (sides of the channel) to -40 deg at the center of the channel (Fig. 3.4b,d,f). In terms of tidal propagation, this means that changes occur first at the sides of the channel and then at the center of the channel about two hours later. Equivalent phase difference in along-channel velocity across the channel was found in Lieberthal et al. (2019). Flood and ebb are symmetric (Fig. 3.5), because non-linear terms which cause tidal asymmetry are not included. It is stressed that

along-channel velocity is only a part of the flow within the estuary and the additional components of velocity are examined next.

Across-channel and vertical velocities are at least an order of magnitude less than along-channel velocities within the estuary, as seen in Lieberthal et al (2019).

Across-channel (lateral) velocity is the product of the combined effects of Coriolis, lateral depth-averaged density gradient and the lateral gradient of higher order (first and second) sea level (Eq. (3.4)). The solution for amplitude of across-channel velocity differs slightly from that found in Ensing et al. (2015), but it is not clear at this time if there is a mistake in their derivation. Figure 3.5, shows along-channel velocity (contours) and lateral velocities (vectors) throughout the estuary cross-section at one-quarter length into the estuary and mid-estuary over the tidal cycle. Lateral velocity in the Damariscotta estuary exhibits a two-cell structure. During flood, lateral velocities near the surface flow right, when looking into the estuary towards the head of the estuary, and lateral flow is in the opposite direction near the bottom of the estuary (Fig. 3.5).

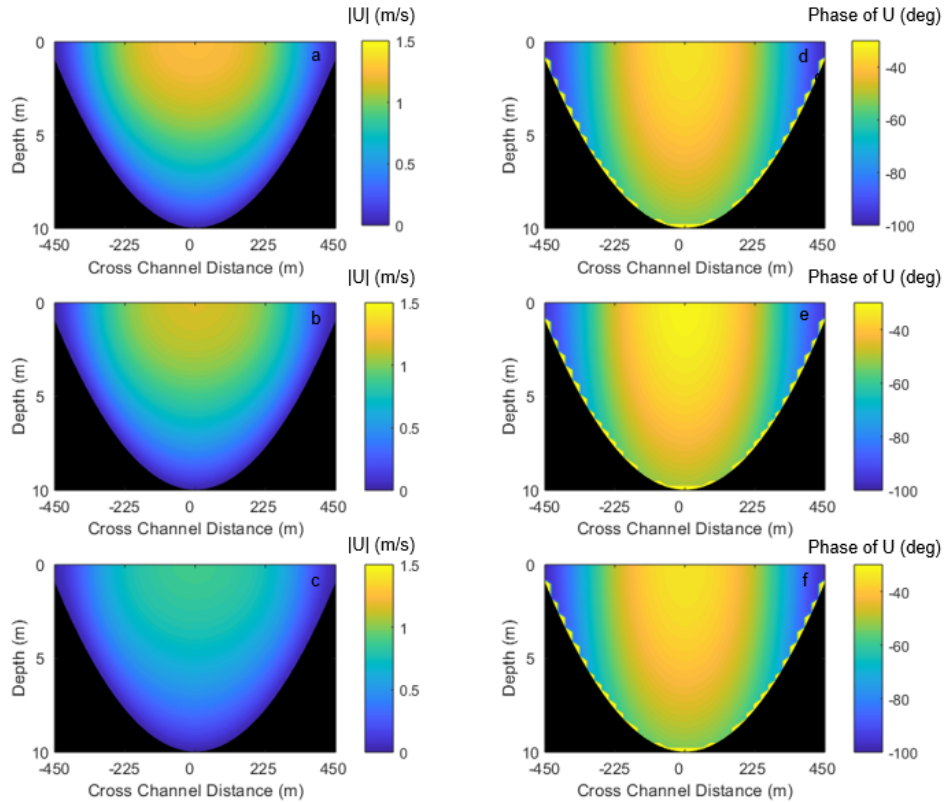


Figure 3.4. Amplitude (a, c, e) and phase (b, d, f) of along-channel velocity, u , at one-quarter length (top row) into the estuary, mid-estuary (middle row), and three-quarters into the estuary (bottom row) for the estuary cross-section. Amplitude (a, c, e) and phase (b, d, f) of along-channel velocity, u , at one-quarter length (top row) into the estuary, mid-estuary (middle row), and three-quarters into the estuary (bottom row) for the estuary cross-section. Across channel position, y is along the x-axis and depth, z , is along the y-axis

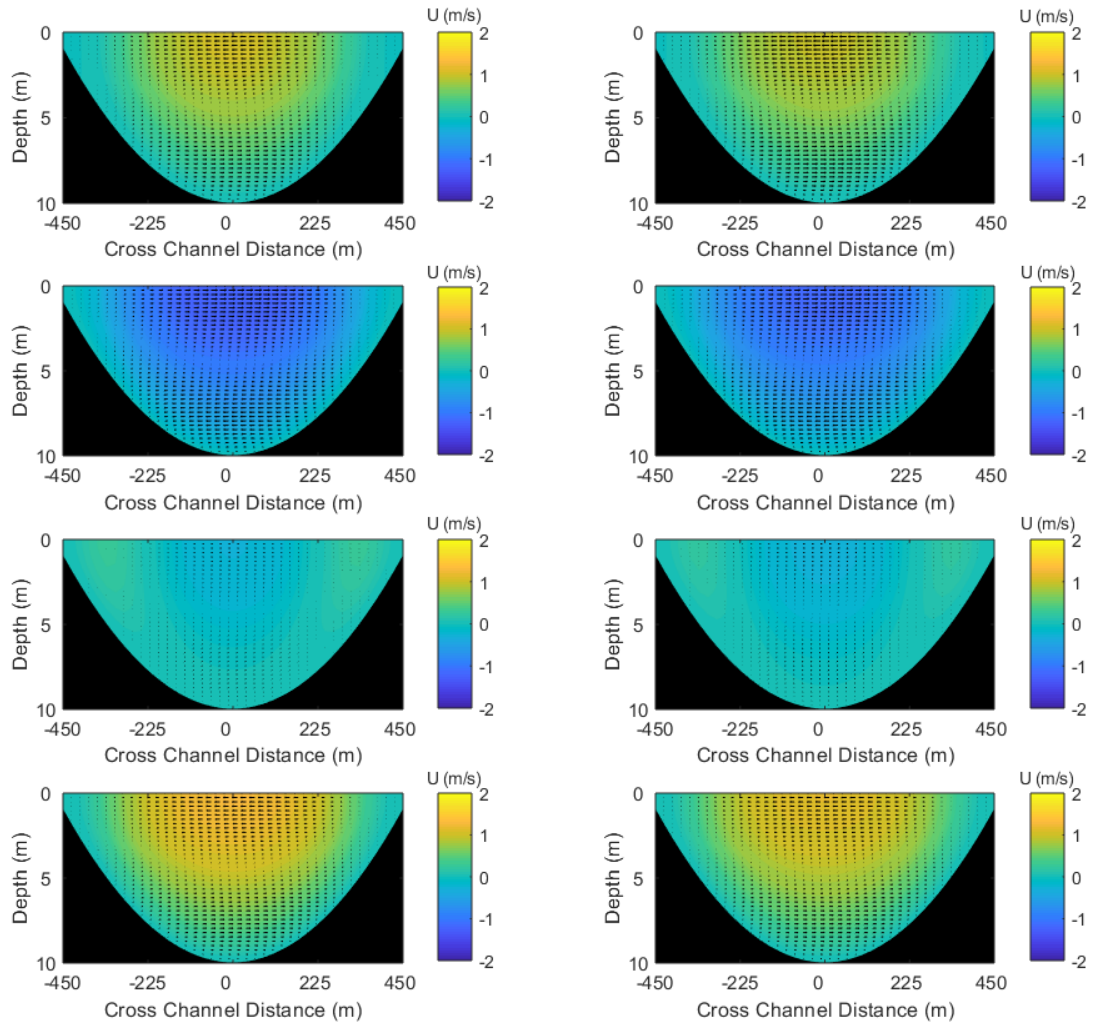


Figure 3.5. Along-channel velocity at one-quarter length (left) and half-length (right) into the estuary during several times during the tidal cycle: $t = 0$ (a,b), $t = 6$ h(c,d), $t = 9$ h (e,f), $t = 11.5$ h (g,h). Along-channel velocity at one-quarter length (left) and half-length (right) into the estuary during several times during the tidal cycle: $t = 0$ (a,b), $t = 6$ h(c,d), $t = 9$ h (e,f), $t = 11.5$ h (g,h). Contours represent along-channel velocity (m/s). Vectors are across-channel velocity (m/s).

3.3 Sensitivity to Friction and Width Convergence

In this section, sensitivity of water level elevation and velocity amplitudes to changes in friction and width convergence are investigated by altering the vertical eddy viscosity, A_v , and the width convergence factor, μ . First, we consider friction. When friction is increased ($A_v = 10^{-1}$), water level elevation decreases into the estuary until width convergence becomes more important and water level increases slightly towards the head of the estuary, while when friction is weaker ($A_v = 10^{-4}$) water level elevation is amplified by width convergence throughout the estuary (Fig. 3.6a, b). Amplitude of along-channel is diminished towards the estuary by strong friction (Fig. 3.7a). For weaker friction, the maximum amplitude of along-channel velocity is an order of magnitude greater than for normal friction within the Damariscotta estuary and along-channel velocity, although initially amplified slightly, decreases towards the head of the estuary (Fig.3.7b). Although, not presented here, weaker friction leads to a subsurface maximum in along-channel velocity, because interaction with the boundaries has weaker effect. The convergence factor of the Damariscotta estuary, $\mu \approx 0.5$, is relatively weak width convergence, so only strong convergence is considered in this section. Strong convergence ($\mu = 3$) leads to amplification of amplitudes of water level elevation and along-channel velocity along the estuary (Fig. 3.8).

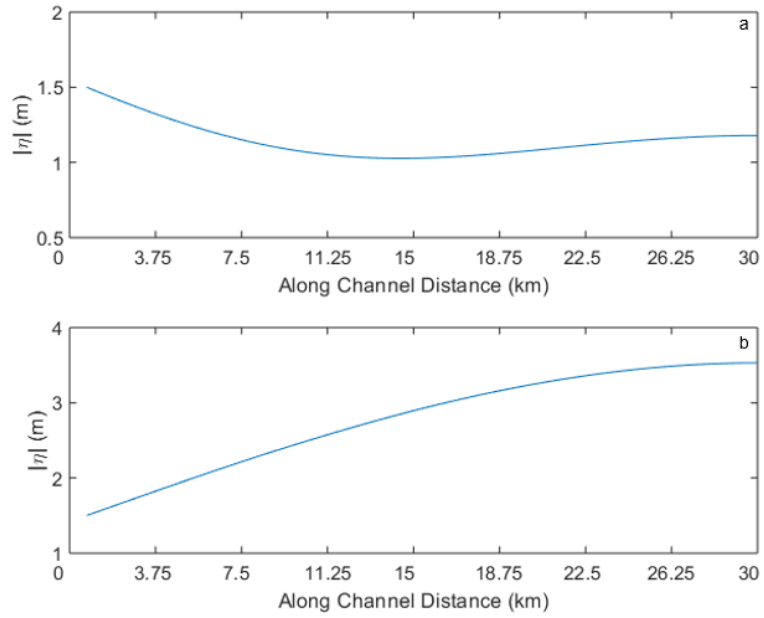


Figure 3.6. Amplitude of water level (η) for vertical eddy viscosity, A_v , values of 10^{-1} (a) and 10^{-4} (b), representative of strong and weak friction, respectively. Amplitude of water level(η) for vertical eddy viscosity, A_v , values of 10^{-1} (a) and 10^{-4} (b), representative of strong and weak friction, respectively.

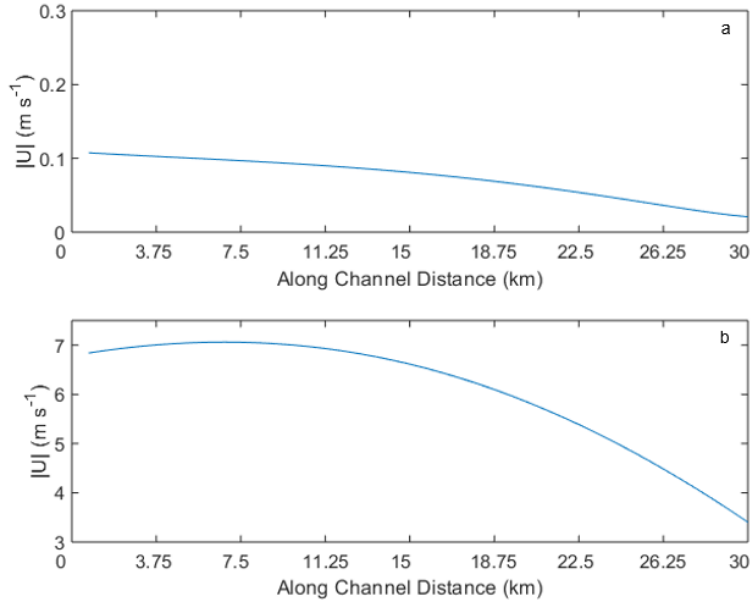


Figure 3.7. Amplitude of along-channel velocity (u) for vertical eddy viscosity, A_v , values of 10^{-1} (a) and 10^{-4} (b), representative of strong and weak friction, respectively.

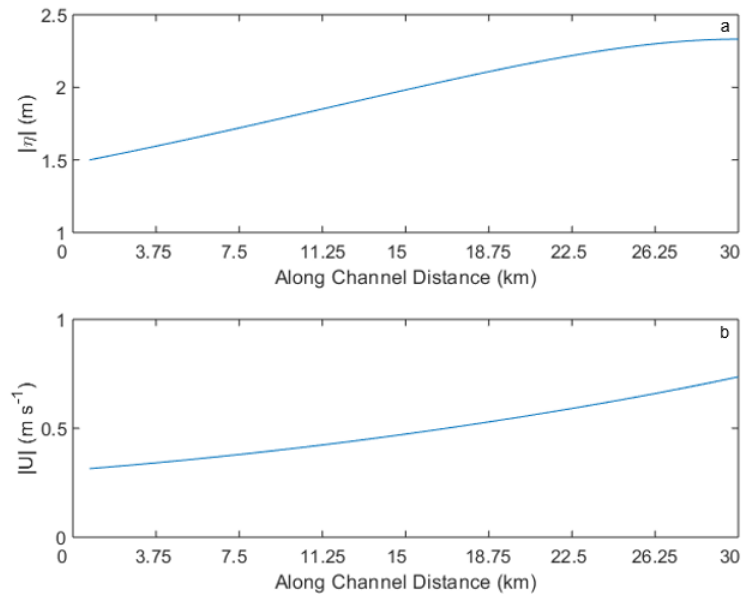


Figure 3.8. Amplitude of water level (a) and along-channel velocity (b) for a channel with stronger width convergence, $\mu = 3$.

3.4 Significance, Limitations, and Future Work

This thesis expands on the spatial scale of [7], which investigated one interesting section of the Damariscotta estuary, by providing results for the entire length. The solutions found for across-channel velocity and the higher order sea level gradient are unique, although derived as in [4]. The model has several limitations. First, the model is only able to study tidal flow, excluding residual flow. The first order solution, which represents the residual flow, is complicated to solve analytically. Non-linear terms, which are responsible for tidal asymmetry, are excluded from the model so flood or ebb dominance within the Damariscotta Estuary cannot be determined by this study. Friction is considered to be constant with depth, but in an estuary friction varies significantly with depth. The solution becomes more complicated, however, if friction is not considered constant. These, in combination, could explain discrepancies between model results and observational data. Future work should focus on the residual flow within the estuary and include the effects of non-linear terms and variable friction. However, this may have to be done numerically, as the problem may be too difficult to solve through analytical methods.

3.5 Conclusions

This thesis derives a three-dimensional analytical model by perturbation expansion of the Navier-Stokes equations in the shallow water limit, modified from Ensing et al. (2015). The resulting zero-order solution is analyzed to provide insight into the tidal flow of the tidally-dominated, well-mixed Damariscotta River Estuary. The water level elevation, and flow velocity in three-dimensions are presented after applying the model with parameters representative of the properties of the Damariscotta estuary. Parameters for friction and width convergence are then changed to investigate the sensitivity of the estuary to those forces. Water level elevation amplitude increases into the estuary due to amplification by width convergence, and along-channel velocity amplitude decreased into the estuary due to dampening by friction. This phenomenon suggests width convergence has greater influence

on water level elevation, whereas friction is more influential to velocity. Lateral velocities exhibited a two cell structure with flow of the near-surface cell and the near-bottom cell in opposite directions. Results of the model compared well to previous studies within the estuary [7] and to the Upper Ems estuary [4] , which has similar dynamics as the Damariscotta estuary although important morphological distinctions should be noted. Tidal asymmetry and variable friction within the estuary were not studied in this thesis, as non-linear terms were dropped in governing equations and vertical eddy viscosity was assumed to be constant. Furthermore, the model considers the zero-order solution and is unable to study residual flow in the estuary. Future work should investigate tidal asymmetry and residual flow in the Damariscotta estuary, while considering a more complicated friction regime.

REFERENCES

- [1] W M. Cameron and D W. Pritchard. Estuaries (306–324). *The Sea*, 2, 1963.
- [2] J Dronkers. Tidal asymmetry and estuarine morphology. *Netherlands Journal of Sea Research*, 20(2-3):117–131, 1986.
- [3] K R. Dyer. *Estuaries: a physical introduction*. John Wiley, 2 edition, 1997.
- [4] E Ensing, H E. de Swart, and H M. Schuttelaars. Sensitivity of tidal motion in well-mixed estuaries to cross-sectional shape, deepening, and sea level rise. *Ocean Dynamics*, 65(7):933–950, 2015.
- [5] C T. Friedrichs and D G. Aubrey. Non-linear tidal distortion in shallow well-mixed estuaries: a synthesis. *Estuarine, Coastal and Shelf Science*, 27(5):521–545, 1988.
- [6] C T. Friedrichs and D G. Aubrey. Tidal propagation in strongly convergent channels. *Journal of Geophysical Research: Oceans*, 99(C2):3321–3336, 1994.
- [7] B Lieberthal, K Huguenard, L Ross, and K Bears. The generation of overtides in flow around a headland in a low inflow estuary. *Journal of Geophysical Research: Oceans*, 124(2):955–980, 2019.
- [8] L M. Mayer, D W. Townsend, N R. Pettigrew, T C. Loder, M W. Wong, D Kistner-Morris, A K. Laursen, A D. Schoudel, C Conairis, J Brown, et al. The Kennebec, Sheepscot and Damariscotta River estuaries: Seasonal oceanographic data. University of Maine. Technical report, Department of Oceanography Technical Report, 1996.
- [9] B J. McAlice. A preliminary oceanographic survey of the Damariscotta River estuary, Lincoln County, Maine. *Maine Sea Grant Technical Report*, 1977.
- [10] M M. Nichols and R B. Biggs. Estuaries in: Davis ra (ed) coastal sedimentary environments, 77–186, 1985.
- [11] D W. Pritchard. Salinity distribution and circulation in the Chesapeake Bay estuarine system.. 1. *Mar. Res*, 11:106–123, 1952.
- [12] L Ross, H de Swart, E Ensing, and A Valle-Levinson. Three-dimensional tidal flow in a fjord-like basin with converging width: An analytical model. *Journal of Geophysical Research: Oceans*, 122(9):7558–7576, 2017.
- [13] P E. Speer and D G. Aubrey. A study of non-linear tidal propagation in shallow inlet/estuarine systems part ii: Theory. *Estuarine, Coastal and Shelf Science*, 21(2):207–224, 1985.
- [14] A Valle-Levinson. Definition and classification of estuaries. *Contemporary issues in estuarine physics*, 1:1–10, 2010.

- [15] C D. Winant. Three-dimensional tidal flow in an elongated, rotating basin. *Journal of Physical Oceanography*, 37(9):2345–2362, 2007.

BIOGRAPHY OF THE AUTHOR

Stephanie Ayres was born and raised in Maryland. She attended University of South Carolina for undergraduate studies in marine science with an emphasis in physical oceanography and a minor in mathematics. She obtained a M.S. in Oceanography from the University of Maine in 2017. Her thesis focused on developing a method to directly measure the cell density of marine diatoms. Stephanie Lauren Ayres is a candidate for the Master of Arts degree in Mathematics from the University of Maine in December 2019.